26

Electromagnetic radiation from sources in an unbounded, homogeneous, isotropic medium

In this chapter we calculate the electromagnetic field that is causally related to the action of exciting sources of bounded extent in an unbounded homogeneous, isotropic medium that is linear, time invariant and locally reacting in its electromagnetic behaviour. The field quantities (electric field strength and magnetic field strength) are determined with the aid of a spatial Fourier transformation method that is applied to the complex frequency-domain equations that have been discussed in Chapter 24. The electric-current and the magnetic-current source vector potentials are introduced. Several applications are given. In particular, the radiation from current-carrying wire segments and current-carrying loops is discussed, both in the complex frequency domain and in the space–time domain. Finally, the solution to the initial-value problem (Cauchy problem) for a lossless medium is given.

26.1 The electromagnetic field equations and their solution in the angular wave-vector domain

The complex frequency-domain electric and magnetic field strengths $\hat{E}_r$ and $\hat{H}_p$ in a homogeneous and isotropic medium satisfy the complex frequency-domain electromagnetic field equations (see Equations (24.4-1) and (24.4-2))

$$-\varepsilon_{k,m,p}\partial_m\hat{H}_p + \hat{\eta}\hat{E}_k = -\hat{J}_k\,, \tag{26.1-1}$$

$$\varepsilon_{j,n,r}\partial_n\hat{E}_r + \hat{\zeta}\hat{H}_j = -\hat{K}_j\,, \tag{26.1-2}$$

in which the transverse admittance $\hat{\eta}$ and the longitudinal impedance $\hat{\zeta}$ per length of the medium are given by

$$\hat{\eta} = \hat{\sigma} + s\hat{\varepsilon}\,, \tag{26.1-3}$$

$$\hat{\zeta} = s\hat{\mu}\,, \tag{26.1-4}$$

for a medium with relaxation, by

$$\hat{\eta} = s\varepsilon\,, \tag{26.1-5}$$

$$\hat{\xi} = s\mu\,, \tag{26.1-6}$$

for an instantaneously reacting (i.e. lossless) medium, and by

$$\hat{\eta} = \sigma + s\varepsilon\,, \tag{26.1-7}$$

$$\hat{\xi} = \Gamma + s\mu\,, \tag{26.1-8}$$

for a medium with conductive electric and linear magnetic hysteresis losses. (In many applications, the magnetic hysteresis losses are negligible and Γ can be put equal to zero. However, the inclusion of Γ in the formulas makes these symmetrical in the electric and the magnetic properties, which is an important check in all mathematical expressions related to the electromagnetic field.) A particular case of a medium with relaxation which we shall consider, is the collisionless electron plasma and the superconducting metal, for which

$$\hat{\eta} = s\varepsilon_0(1 + \omega_{pe}^2/s^2)\,, \tag{26.1-9}$$

$$\hat{\xi} = s\mu_0\,, \tag{26.1-10}$$

Since the medium is homogeneous, $\hat{\eta} = \hat{\eta}(s)$ and $\hat{\xi} = \hat{\xi}(s)$ are independent of position. We assume that the volume source density of electric current $\hat{J}_k$ and the volume source density of magnetic current $\hat{K}_j$ only differ from zero in some bounded subdomain $\mathcal{D}^T$ of $\mathcal{R}^3$; $\mathcal{D}^T$ is the *spatial support* of the source distributions and is denoted as the *source domain* of the radiated (or transmitted) field (Figure 26.1-1). The influence of non-zero initial field values has been incorporated into the volume source densities.

To solve Equations (26.1-1) and (26.1-2) we subject these equations to a three-dimensional Fourier transformation over the entire configuration space $\mathcal{R}^3$ (see Section B.2). The usefulness of this operation is associated with the property of shift invariance of the medium in all Cartesian directions. In accordance with Appendix B the spatial Fourier transformation is written as

$$\{\tilde{E}_r,\tilde{H}_p\}(\mathrm{j}k,s) = \int_{x\in\mathcal{R}^3} \exp(\mathrm{j}k_s x_s)\{\hat{E}_r,\hat{H}_p\}(x,s)\,\mathrm{d}V\,, \tag{26.1-11}$$

where j denotes the imaginary unit and

$$k = k_1 i(1) + k_2 i(2) + k_3 i(3) \qquad \text{with} \quad k\in\mathcal{R}^3\,, \tag{26.1-12}$$

is the *angular wave vector* in three-dimensional Fourier-transform or k-space. According to Fourier's theorem we inversely have

$$\{\hat{E}_r,\hat{H}_p\}(x,s) = (2\pi)^{-3}\int_{k\in\mathcal{R}^3} \exp(-\mathrm{j}k_s x_s)\{\tilde{E}_r,\tilde{H}_p\}(\mathrm{j}k,s)\,\mathrm{d}V\,. \tag{26.1-13}$$

For the spatial derivatives we employ the relation

$$\int_{x\in\mathcal{R}^3} \exp(\mathrm{j}k_s x_s)\partial_m\{\hat{E}_r,\hat{H}_p\}(x,s)\,\mathrm{d}V = -\mathrm{j}k_m\{\tilde{E}_r,\tilde{H}_p\}(\mathrm{j}k,s)\,, \tag{26.1-14}$$

where it has been taken into account that $\hat{E}_r$ and $\hat{H}_p$ will, due to causality, show, for $\mathrm{Re}(s) > 0$, an exponential decay as $|x|\to\infty$. (In Section 26.3 this will be shown indeed to be true.) With this, Equations (26.1-1) and (26.1-2) transform into

$$\mathrm{j}k_m\varepsilon_{k,m,p}\tilde{H}_p + \hat{\eta}\tilde{E}_k = -\tilde{J}_k\,, \tag{26.1-15}$$

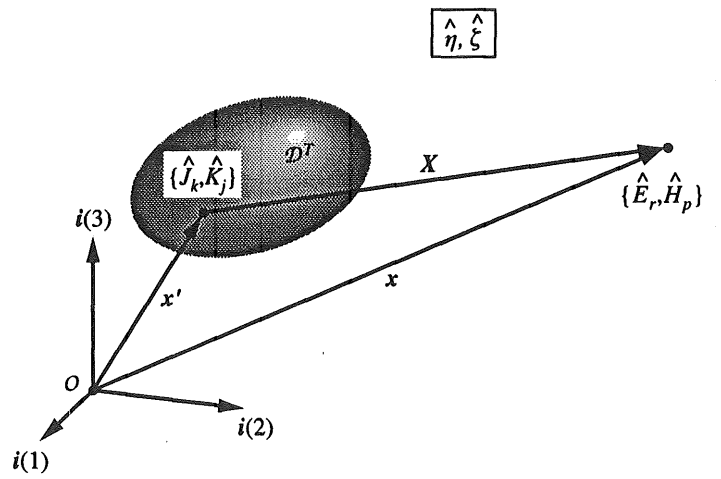

Figure 26.1-1 Sources $\{\hat{J}_k, \hat{K}_j\}$ at position $x' \in \mathcal{D}^T$ (source domain) generate electromagnetic radiation in a homogeneous, isotropic medium with complex frequency-domain electromagnetic parameters $\{\hat{\eta}, \hat{\zeta}\}$. The field $\{\hat{E}_r, \hat{H}_p\}$ is observed at position $x \in \mathcal{R}^3$.

$$-\mathrm{j}k_n \varepsilon_{j,n,r} \tilde{E}_r + \hat{\zeta} \tilde{H}_j = -\tilde{K}_j \,, \tag{26.1-16}$$

where

$$\{\tilde{J}_k, \tilde{K}_j\}(\mathrm{j}k, s) = \int_{x \in \mathcal{D}^T} \exp(\mathrm{j}k_s x_s) \{\hat{J}_k, \hat{K}_j\}(x, s) \, \mathrm{d}V \tag{26.1-17}$$

is the spatial Fourier transform of the source distributions. (Note that the integration on the right-hand side is extended over the source domain $\mathcal{D}^T$.) Multiplication of Equation (26.1-15) by k_k and taking into account that $k_k k_m \varepsilon_{k,m,p} = 0$ in view of the antisymmetry of $\varepsilon_{k,m,p}$ in its subscripts k and m, leads to the compatibility relation in angular wave-vector space

$$\hat{\eta} k_k \tilde{E}_k = -k_k \tilde{J}_k \,. \tag{26.1-18}$$

Similarly, multiplication of Equation (26.1-16) by k_j and taking into account that $k_j k_n \varepsilon_{j,n,r} = 0$ in view of the antisymmetry of $\varepsilon_{j,n,r}$ in its subscripts j and n, leads to the compatibility relation in angular wave-vector space

$$\hat{\zeta} k_j \tilde{H}_j = -k_j \tilde{K}_j \,. \tag{26.1-19}$$

To solve $\{\tilde{E}_r, \tilde{H}_p\}$ from Equations (26.1-15) and (26.1-16) we first eliminate one of the angular wave-vector domain field quantities. For example, $\tilde{H}_p$ is first eliminated. To this end, $\tilde{H}_j$ is solved from Equation (26.1-16) to yield

$$\tilde{H}_j = \hat{\zeta}^{-1} (\mathrm{j}k_n \varepsilon_{j,n,r} \tilde{E}_r - \tilde{K}_j) \,. \tag{26.1-20}$$

Replacing the subscript j by p, substituting the result in Equation (26.1-15) and multiplying through by $\hat{\zeta}$, the following equation for the electric field strength in angular wave-vector space is obtained

$$\mathrm{j}k_m \varepsilon_{k,m,p} \mathrm{j}k_n \varepsilon_{p,n,r} \tilde{E}_r + \hat{\eta} \hat{\zeta} \tilde{E}_k = -\hat{\zeta} \tilde{J}_k + \mathrm{j}k_m \varepsilon_{k,m,p} \tilde{K}_p \,, \tag{26.1-21}$$

or, employing the relation (see Equation (A.7-51))

$$\varepsilon_{k,m,p}\varepsilon_{p,n,r} = \delta_{k,n}\delta_{m,r} - \delta_{k,r}\delta_{m,n}\,, \tag{26.1-22}$$

the equation

$$-k_k k_r \tilde{E}_r + k_m k_m \tilde{E}_k + \hat{\eta}\hat{\xi}\tilde{E}_k = -\hat{\xi}\tilde{J}_k + \mathrm{j}k_m \varepsilon_{k,m,p}\tilde{K}_p\,. \tag{26.1-23}$$

Now, Equation (26.1-23) would be simple to solve if we had a known expression for $k_r\tilde{E}_r$. Such an expression is provided by the compatibility relation of Equation (26.1-18). Use of Equation (26.1-18) in Equation (26.1-23) leads to

$$(k_m k_m + \hat{\eta}\hat{\xi})\tilde{E}_k = -\hat{\xi}\tilde{J}_k - \hat{\eta}^{-1}k_k k_r \tilde{J}_r + \mathrm{j}k_m \varepsilon_{k,m,p}\tilde{K}_p\,. \tag{26.1-24}$$

From Equation (26.1-24) the expression for the electric field strength in angular wave-vector space is obtained as

$$\tilde{E}_k = \tilde{G}(-\hat{\xi}\tilde{J}_k - \hat{\eta}^{-1}k_k k_r \tilde{J}_r + \mathrm{j}k_m \varepsilon_{k,m,p}\tilde{K}_p)\,, \tag{26.1-25}$$

in which $\tilde{G}$ is given by

$$\tilde{G} = \frac{1}{k_m k_m + \hat{\eta}\hat{\xi}}\,. \tag{26.1-26}$$

A similar procedure is employed to determine the expression for the magnetic field strength in angular wave-vector space. For this, $\tilde{E}_r$ is eliminated from Equations (26.1-15) and (26.1-16). To this end, $\tilde{E}_k$ is solved from Equation (26.1-15) to yield

$$\tilde{E}_k = -\hat{\eta}^{-1}(\mathrm{j}k_m \varepsilon_{k,m,p}\tilde{H}_p + \tilde{J}_k)\,. \tag{26.1-27}$$

Replacing the subscript k by r, substituting the result in Equation (26.1-16) and multiplying through by $\hat{\eta}$, the following equation for the magnetic field strength in angular wave-vector space is obtained

$$\mathrm{j}k_n \varepsilon_{j,n,r}\mathrm{j}k_m \varepsilon_{r,m,p}\tilde{H}_p + \hat{\eta}\hat{\xi}\tilde{H}_j = -\hat{\eta}\tilde{K}_j - \mathrm{j}k_n \varepsilon_{j,n,r}\tilde{J}_r\,, \tag{26.1-28}$$

or, employing the relation (see Equation (A.7-51))

$$\varepsilon_{j,n,r}\varepsilon_{r,m,p} = \delta_{j,m}\delta_{n,p} - \delta_{j,p}\delta_{n,m}\,, \tag{26.1-29}$$

the equation

$$-k_j k_p \tilde{H}_p + k_n k_n \tilde{H}_j + \hat{\eta}\hat{\xi}\tilde{H}_j = -\hat{\eta}\tilde{K}_j - \mathrm{j}k_n \varepsilon_{j,n,r}\tilde{J}_r\,. \tag{26.1-30}$$

Now, Equation (26.1-30) would be simple to solve if we had a known expression for $k_p\tilde{H}_p$. Such an expression is provided by the compatibility relation of Equation (26.1-19). Use of Equation (26.1-19) in Equation (26.1-30) leads to

$$\tilde{H}_j = \tilde{G}(-\hat{\eta}\tilde{K}_j - \hat{\zeta}^{-1}k_j k_p \tilde{K}_p - \mathrm{j}k_n \varepsilon_{j,n,r}\tilde{J}_r)\,, \tag{26.1-31}$$

in which $\tilde{G}$ is given by Equation (26.1-26).

To elucidate the structural dependence of the fields on the source distributions that generate them, we introduce the angular wave-vector domain electric-current source vector potential

$$\tilde{\Phi}_k^J = \tilde{G}\tilde{J}_k \tag{26.1-32}$$

and the angular wave-vector domain magnetic-current source vector potential

$$\tilde{\Phi}_j^K = \tilde{G}\tilde{K}_j . \tag{26.1-33}$$

In terms of these, Equation (26.1-25) can be rewritten as

$$\tilde{E}_k = -\hat{\zeta}\tilde{\Phi}_k^J - \hat{\eta}^{-1}k_k k_r \tilde{\Phi}_r^J + \mathrm{j}k_m \varepsilon_{k,m,p}\tilde{\Phi}_p^K , \tag{26.1-34}$$

and Equation (26.1-31) as

$$\tilde{H}_j = -\hat{\eta}\tilde{\Phi}_j^K - \hat{\zeta}^{-1}k_j k_p \tilde{\Phi}_p^K - \mathrm{j}k_n \varepsilon_{j,n,r}\tilde{\Phi}_r^J . \tag{26.1-35}$$

In Sections 26.2 and 26.3 the inverse spatial Fourier transformation of Equations (26.1-32)–(26.1-35) will be carried out; this will result into the complex frequency-domain expressions for the electric and the magnetic field strengths of the field radiated by the sources. Once the function $\hat{G} = \hat{G}(\boldsymbol{x},s)$ that corresponds to $\tilde{G} = \tilde{G}(\mathrm{j}\boldsymbol{k},s)$ has been determined, elementary rules of the spatial Fourier transformation suffice to construct the expressions for the field components. In Section 26.2, $\hat{G} = \hat{G}(\boldsymbol{x},s)$ will be determined by directly evaluating the Fourier inversion integral applied to $\tilde{G} = \tilde{G}(\mathrm{j}\boldsymbol{k},s)$.

26.2 The Green's function of the scalar Helmholtz equation

In this section, the function $\hat{G} = \hat{G}(\boldsymbol{x},s)$ whose angular wave-vector space counterpart $\tilde{G} = \tilde{G}(\mathrm{j}\boldsymbol{k},s)$ has been introduced in Equation (26.1-26) will be determined. This function can be considered as the basic wave function (Green's function) of the scalar Helmholtz equation. The starting point for the evaluation of $\hat{G}$ is the inverse Fourier transformation

$$\hat{G}(\boldsymbol{x},s) = (2\pi)^{-3}\int_{\boldsymbol{k}\in\mathcal{R}^3} \exp(-\mathrm{j}k_s x_s)\tilde{G}(\mathrm{j}\boldsymbol{k},s)\,\mathrm{d}V , \tag{26.2-1}$$

in which

$$\tilde{G}(\mathrm{j}\boldsymbol{k},s) = \frac{1}{k_m k_m + \hat{\gamma}^2} , \tag{26.2-2}$$

with

$$\hat{\gamma} = (\hat{\eta}\hat{\zeta})^{1/2} . \tag{26.2-3}$$

In Equation (26.2-3), $\mathrm{Re}(\hat{\gamma}) > 0$ for $\mathrm{Re}(s) > 0$, since $\hat{\zeta} = \hat{\zeta}(s)$ and $\hat{\eta} = \hat{\eta}(s)$ share this property. By applying the standard rules of the spatial Fourier transformation (see Appendix B), it is easily verified that $\tilde{G} = \tilde{G}(\mathrm{j}\boldsymbol{k},s)$ is the three-dimensional Fourier transform, over the entire configuration space $\mathcal{R}^3$, of the function $\hat{G} = \hat{G}(\boldsymbol{x},s)$ that satisfies the three-dimensional scalar Helmholtz equation with point-source excitation

$$(\partial_m\partial_m - \hat{\gamma}^2)\hat{G} = -\delta(\boldsymbol{x}) , \tag{26.2-4}$$

where $\delta(\boldsymbol{x})$ is the three-dimensional Dirac distribution (impulse function) operative at $\boldsymbol{x} = \boldsymbol{0}$.

The simplest way to evaluate the right-hand side of Equation (26.2-1) is to introduce spherical coordinates in $\boldsymbol{k}$-space with centre at $\boldsymbol{k} = \boldsymbol{0}$ and the direction of $\boldsymbol{x}$ as the polar axis. Let θ be the angle between $\boldsymbol{k}$ and $\boldsymbol{x}$, and ϕ be the angle between the projection of $\boldsymbol{k}$ on the plane perpendicular to $\boldsymbol{x}$ and some fixed direction in this plane (Figure 26.2-1), then the range of integration is $0 \leqslant |\boldsymbol{k}| < \infty$, $0 \leqslant \theta \leqslant \pi$, $0 \leqslant \phi < 2\pi$, while

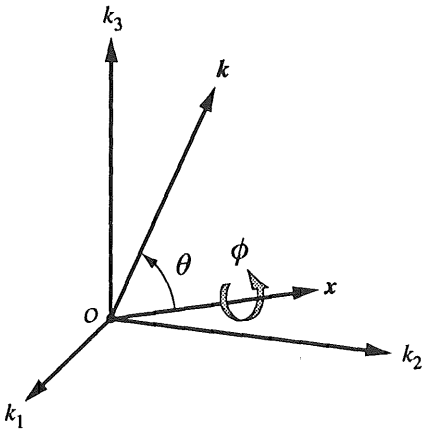

Figure 26.2-1 Integration in k-space to evaluate $\hat{G}(x,s)$; $\{|k|,\theta,\phi\}$ are the spherical polar coordinates, with x as polar axis and the ranges of integration $0 \leq |k| < \infty$, $0 \leq \theta \leq \pi$, $0 \leq \phi < 2\pi$.

$$k_s x_s = |k||x| \cos(\theta)\,, \tag{26.2-5}$$

$$k_m k_m = |k|^2\,, \tag{26.2-6}$$

and

$$dV = |k|^2 \sin(\theta)\, d|k|\, d\theta\, d\phi\,. \tag{26.2-7}$$

In the resulting right-hand side of Equation (26.2-1) we first carry out the integration with respect to ϕ. Since the integrand is independent of ϕ, this merely amounts to a multiplication by a factor of 2π. Next, we carry out the integration with respect to θ, which is elementary. After this we have, for $|x| \neq 0$,

$$\hat{G}(x,s) = \frac{1}{4\pi^2} \int_{|k|=0}^{\infty} \frac{|k|^2}{|k|^2 + \hat{\gamma}^2} \left[\frac{\exp[-\mathrm{j}|k||x| \cos(\theta)]}{\mathrm{j}|k||x|} \right]_{\theta=0}^{\pi} d|k|$$

$$= \frac{1}{4\pi^2 \mathrm{j}|x|} \int_{|k|=0}^{\infty} \frac{\exp(\mathrm{j}|k||x|) - \exp(-\mathrm{j}|k||x|)}{|k|^2 + \hat{\gamma}^2} |k|\, d|k|\,. \tag{26.2-8}$$

Considering $|k|$ as a variable that can take on arbitrary complex values and denoting this variable by k, Equation (26.2-8) can be rewritten as

$$\hat{G}(x,s) = -\frac{1}{4\pi^2 \mathrm{j}|x|} \int_{k=-\infty}^{\infty} \frac{\exp(-\mathrm{j}k|x|)}{k^2 + \hat{\gamma}^2} k\, dk\,. \tag{26.2-9}$$

The integral on the right-hand side of Equation (26.2-9) is evaluated by continuing the integrand analytically into the complex k plane, supplementing the path of integration by a semi-circle situated in the lower half-plane $-\infty < \mathrm{Im}(k) \leq 0$ and of infinitely large radius, and applying the theorem of residues (Figure 26.2-2). On account of Jordan's lemma, the contribution from the semi-circle at infinity vanishes. Furthermore, the only singularity of the integrand in the lower

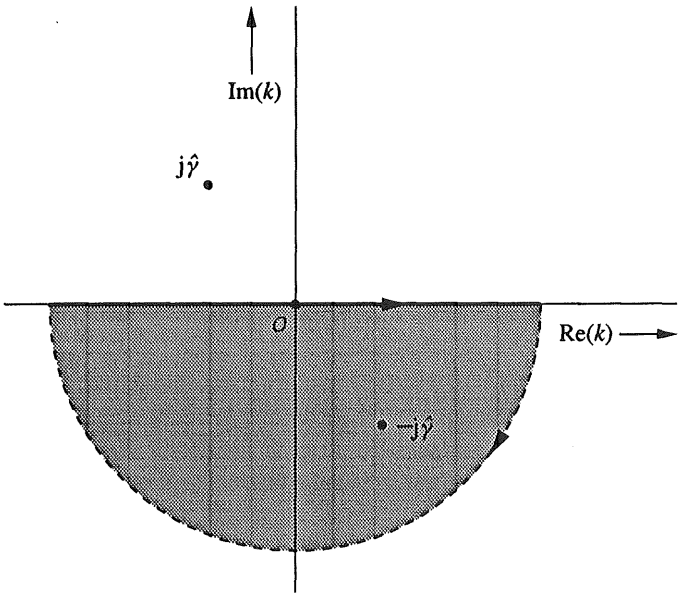

Figure 26.2-2 Integration in the complex k plane to evaluate $\hat{G}(x,s)$. Jordan's lemma and the theorem of residues are applied to the closed contour in the lower half-plane, where $\mathrm{Im}(k) < 0$. The simple pole in the lower half-plane is located at $k = -j\hat{\gamma}$, since $\mathrm{Re}(\hat{\gamma}) > 0$ for $\mathrm{Re}(s) > 0$.

half of the complex k plane is the simple pole at $k = -j\hat{\gamma}$ (note that $\mathrm{Re}(\hat{\gamma}) > 0$ for $\mathrm{Re}(s) > 0$). Taking into account the residue of this pole and the fact that the contour integration is carried out clockwise instead of counter-clockwise, we arrive at

$$\hat{G}(x,s) = \exp(-\hat{\gamma}|x|)/4\pi|x| \qquad \text{for } |x| \neq 0\,. \tag{26.2-10}$$

This expression will be used in the process of inversely Fourier transforming the angular wave-vector domain wave quantities obtained in Section 26.1.

In the course of our further analysis we also need the first- and second-order spatial derivatives of $\hat{G}$. By straightforward differentiation these are obtained from Equations (26.2-10) as

$$\partial_m \hat{G}(x,s) = \frac{1}{4\pi}\left(-\frac{1}{|x|^2} - \frac{\hat{\gamma}}{|x|}\right)\frac{x_m}{|x|}\exp(-\hat{\gamma}|x|) \qquad \text{for } |x| \neq 0\,, \tag{26.2-11}$$

and

$$\partial_k \partial_r \hat{G}(x,s) = \frac{1}{4\pi}\left[\frac{1}{|x|^3}\left(\frac{3x_k x_r}{|x|^2} - \delta_{k,r}\right) + \frac{\hat{\gamma}}{|x|^2}\left(\frac{3x_k x_r}{|x|^2} - \delta_{k,r}\right) + \frac{\hat{\gamma}^2}{|x|}\frac{x_k x_r}{|x|^2}\right]\exp(-\hat{\gamma}|x|)$$

$$\text{for } |x| \neq 0\,. \tag{26.2-12}$$

These results will be used in our subsequent analysis.

Exercises

Exercise 26.2-1

Prove, by using Equation (26.2-2) and carrying out in the relevant Fourier integral a contour integration in the complex k_3 plane, that

$$\hat{G}(x,s) = \exp(-\hat{\gamma}|x|)/4\pi|x| = \left(\frac{1}{2\pi}\right)^2 \int_{\{k_1,k_2\}\in\mathcal{R}^2} \frac{\exp\left[-\mathrm{j}(k_1x_1 + k_2x_2) - (k_1^2 + k_2^2 + \hat{\gamma}^2)^{1/2}|x_3|\right]}{2(k_1^2 + k_2^2 + \gamma^2)^{1/2}} \, \mathrm{d}k_1\mathrm{d}k_2 \,. \quad (26.2\text{-}13)$$

(*Hint*: Observe that $k_3 = \pm\mathrm{j}(k_1^2 + k_2^2 + \hat{\gamma}^2)^{1/2}$ are simple poles of the analytically continued integrand (away from the real k_3 axis) in the upper and lower halves of the complex k_3 plane and that Jordan's lemma applies to a semi-circle in the lower half of the k_3 plane for $x_3 > 0$ and to a semi-circle in the upper half of the k_3 plane for $x_3 < 0$.) (The representation of Equation (26.2-13) plays a major role in the analysis of electromagnetic radiation problems in subdomains of $\mathcal{R}^3$ with parallel, planar, boundaries.)

26.3 The complex frequency-domain source-type representations for the electric and the magnetic field strengths

The complex frequency-domain source-type representations for the electric and the magnetic field strengths of the field radiated by the sources located in $\mathcal{D}^T$ are obtained by carrying out the inverse spatial Fourier transformation to the angular wave-vector domain expressions obtained in Equations (26.1-34) and (26.1-35). Using the rule that $-\mathrm{j}k_m$ corresponds to ∂_m (see Equation (26.1-14)), we obtain

$$\hat{E}_k = -\hat{\zeta}\hat{\Phi}_k^J + \hat{\eta}^{-1}\partial_k\partial_r\hat{\Phi}_r^J - \varepsilon_{k,m,p}\partial_m\hat{\Phi}_p^K, \quad (26.3\text{-}1)$$

and

$$\hat{H}_j = -\hat{\eta}\hat{\Phi}_j^K + \hat{\zeta}^{-1}\partial_j\partial_p\hat{\Phi}_p^K + \varepsilon_{j,n,r}\partial_n\hat{\Phi}_r^J. \quad (26.3\text{-}2)$$

The expressions for the complex frequency-domain electric-current and magnetic-current source vector potentials $\hat{\Phi}_k^J$ and $\hat{\Phi}_j^K$ are obtained by carrying out the inverse spatial Fourier transformation of Equations (26.1-32) and (26.1-33), respectively. Since the product of two functions in angular wave-vector space corresponds to the convolution of these functions in configuration space (see Equations (B.2-11) and (B.2-12)), we obtain

$$\hat{\Phi}_k^J(x,s) = \int_{x'\in\mathcal{D}^T} \hat{G}(x-x',s)\hat{J}_k(x',s)\,\mathrm{d}V \quad (26.3\text{-}3)$$

and

$$\hat{\Phi}_j^K(x,s) = \int_{x'\in\mathcal{D}^T} \hat{G}(x-x',s)\hat{K}_j(x',s)\,\mathrm{d}V, \quad (26.3\text{-}4)$$

in which (see Equation (26.2-10))

$$\hat{G}(x,s) = \exp(-\hat{\gamma}|x|)/4\pi|x| \qquad \text{for} \quad |x| \neq 0\,, \tag{26.3-5}$$

with (see Equation (26.2-3))

$$\hat{\gamma} = (\hat{\eta}\hat{\xi})^{1/2}\,. \tag{26.3-6}$$

Note that in the right-hand sides of Equations (26.3-3) and (26.3-4) we have taken care to distribute the arguments over the functions such that the integration is carried out over the fixed source domain $\mathcal{D}^T$ (see Figure 26.3-1). (If we had provided the source distributions with the argument $x - x'$ and the Green's functions with the argument x', we would have to integrate over a domain that varies with x.)

Equations (26.3-1)–(26.3-6) constitute the solution to the complex frequency-domain electromagnetic radiation problem in an unbounded unhomogeneous, isotropic medium. The expressions are used in the calculation and computation of multitudinous electromagnetic radiation problems. In a number of simple cases, the integrals in Equations (26.3-3) and (26.3-4) can be calculated analytically, and the subsequent differentiations in Equations (26.3-1) and (26.3-2) can be carried out analytically as well. In more complicated cases, the integrals in Equations (26.3-3) and (26.3-4) must be computed with the aid of numerical methods. Since, however, numerical integration can be carried out with almost any desired degree of accuracy, such an evaluation presents, apart from the singularity in $\hat{G}$ at $x' = x$ no difficulties. Numerical differentiation, however, is much more difficult and inherently of restricted accuracy. Therefore, it is in general advantageous to carry out all differentiations in Equations (26.3-1) and (26.3-2) analytically, which can be done since they act on the position vector x that occurs in the argument of $\hat{G}$ (see Equations (26.3-3) and (26.3-4)) only. After having done this, only integrals remain to be evaluated numerically. The relevant derivatives have been evaluated already in Equations (26.2-11) and (26.2-12).

The carrying out of the spatial differentiations in Equations (26.3-1) and (26.3-2) has different consequences for the propagation factor $\exp(-\hat{\gamma}|x - x'|)$ from source point to observation point and the (inverse) powers of the distance decay from source point to observation point. As regards the latter, it will be shown below that the following three types of terms occur:

(a) Terms proportional to (distance)$^{-3}$; these terms represent the *near field* (also denoted as the quasi-static field).

(b) Terms proportional to (distance)$^{-2}$; these terms represent the *intermediate field* (also denoted as the induction field).

(c) Terms proportional to (distance)$^{-1}$; these terms represent the *far field* (also denoted as the radiation field).

In additon, each term in the expressions for the electric and the magnetic field strength has its own directional characteristic in which only the unit vector in the direction of observation $(x_m - x_m')/|x - x'|$ as viewed from the source point occurs.

Finally, observe that $\hat{E}_r$ and $\hat{H}_p$ indeed show, since $\mathrm{Re}(\hat{\gamma}) > 0$ for $\mathrm{Re}(s) > 0$, an exponential decay as $|x| \to \infty$, as has been assumed in Section 26.1.

In what follows, the near-field, intermediate-field, and far-field contributions will be denoted by the double superscripts NF, IF and FF, respectively. Using Equations (26.2-11) and (26.2-12) in Equations (26.3-1) and (26.3-2) and employing the notations

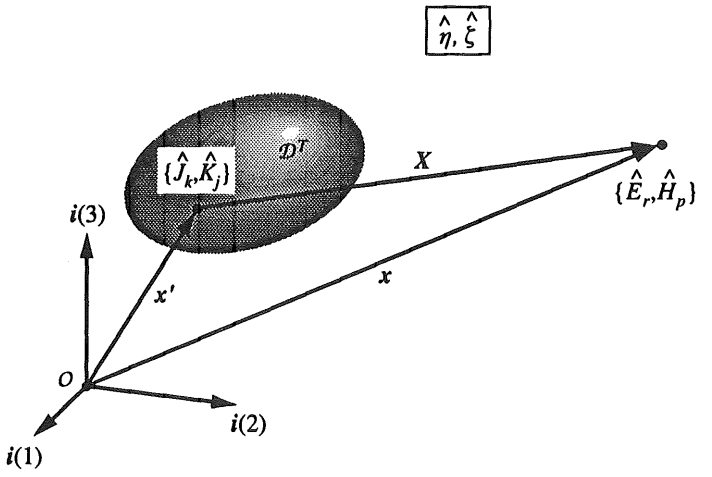

Figure 26.3-1 Complex frequency-domain source-type integral representations for the electromagnetic field $\{\hat{E}_r, \hat{H}_p\}$ observed at position $x \in \mathcal{R}^3$, radiated by sources $\{\hat{J}_k, \hat{K}_j\}$ at position $x \in \mathcal{D}^T$ (bounded source domain) in an unbounded homogeneous, isotropic medium with electromagnetic parameters $\{\hat{\eta}, \hat{\zeta}\}$.

$$X = x - x' \tag{26.3-7}$$

for the position vector from the source point $x' \in \mathcal{D}^T$ to the observation point $x \in \mathcal{R}^3$ and

$$\Xi_m = X_m / |X| \qquad \text{for } |X| \neq 0\,, \tag{26.3-8}$$

for the unit vector along the direction of X (i.e. $\Xi_m \Xi_m = 1$), we arrive at the expressions

$$\hat{E}_k = \hat{E}_k^{\mathrm{NF}} + \hat{E}_k^{\mathrm{IF}} + \hat{E}_k^{\mathrm{FF}}\,, \tag{26.3-9}$$

and

$$\hat{H}_j = \hat{H}_j^{\mathrm{NF}} + \hat{H}_j^{\mathrm{IF}} + \hat{H}_j^{\mathrm{FF}}\,, \tag{26.3-10}$$

in which

$$\hat{E}_k^{\mathrm{NF}}(x,s) = \hat{\eta}^{-1} \int_{x' \in \mathcal{D}^T} (3\Xi_k \Xi_r - \delta_{k,r}) \hat{J}_r(x',s) \frac{\exp(-\hat{\gamma}|X|)}{4\pi |X|^3}\, \mathrm{d}V\,, \tag{26.3-11}$$

$$\begin{aligned} \hat{E}_k^{\mathrm{IF}}(x,s) = (\hat{\gamma}/\hat{\eta}) \int_{x' \in \mathcal{D}^T} (3\Xi_k \Xi_r - \delta_{k,r}) \hat{J}_r(x',s) \frac{\exp(-\hat{\gamma}|X|)}{4\pi |X|^2}\, \mathrm{d}V \\ + \varepsilon_{k,m,p} \int_{x' \in \mathcal{D}^T} \Xi_m \hat{K}_p(x',s) \frac{\exp(-\hat{\gamma}|X|)}{4\pi |X|^2}\, \mathrm{d}V\,, \end{aligned} \tag{26.3-12}$$

$$\begin{aligned} \hat{E}_k^{\mathrm{FF}}(x,s) = \hat{\zeta} \int_{x' \in \mathcal{D}^T} (\Xi_k \Xi_r - \delta_{k,r}) \hat{J}_r(x',s) \frac{\exp(-\hat{\gamma}|X|)}{4\pi |X|}\, \mathrm{d}V \\ + \hat{\gamma} \varepsilon_{k,m,p} \int_{x' \in \mathcal{D}^T} \Xi_m \hat{K}_p(x',s) \frac{\exp(-\hat{\gamma}|X|)}{4\pi |X|}\, \mathrm{d}V\,, \end{aligned} \tag{26.3-13}$$

and

$$\hat{H}_j^{\mathrm{NF}}(x,s) = \hat{\zeta}^{-1} \int_{x' \in \mathcal{D}^T} (3\Xi_j \Xi_p - \delta_{j,p}) \hat{K}_p(x',s) \frac{\exp(-\hat{\gamma}|X|)}{4\pi |X|^3} \, \mathrm{d}V, \tag{26.3-14}$$

$$\hat{H}_j^{\mathrm{IF}}(x,s) = (\hat{\gamma}/\hat{\zeta}) \int_{x' \in \mathcal{D}^T} (3\Xi_j \Xi_p - \delta_{j,p}) \hat{K}_p(x',s) \frac{\exp(-\hat{\gamma}|X|)}{4\pi |X|^2} \, \mathrm{d}V$$
$$- \varepsilon_{j,n,r} \int_{x' \in \mathcal{D}^T} \Xi_n \hat{J}_r(x',s) \frac{\exp(-\hat{\gamma}|X|)}{4\pi |X|^2} \, \mathrm{d}V, \tag{26.3-15}$$

$$\hat{H}_j^{\mathrm{FF}}(x,s) = \hat{\eta} \int_{x' \in \mathcal{D}^T} (\Xi_j \Xi_p - \delta_{j,p}) \hat{K}_p(x',s) \frac{\exp(-\hat{\gamma}|X|)}{4\pi |X|} \, \mathrm{d}V$$
$$- \hat{\gamma} \varepsilon_{j,n,r} \int_{x' \in \mathcal{D}^T} \Xi_n \hat{J}_r(x',s) \frac{\exp(-\hat{\gamma}|X|)}{4\pi |X|} \, \mathrm{d}V. \tag{26.3-16}$$

Equations (26.3-9)–(26.3-16) yield the complex frequency-domain electric and magnetic field strength constituents of the electromagnetic field radiated by distributed volume sources of bounded extent in a homogeneous, isotropic medium. In Section 26.9 the expressions will be used to calculate the electromagnetic field radiated by a wire segment of a current-carrying, conducting wire. In Section 26.10 the expressions will be used to calculate the electromagnetic field radiated by a small current-carrying, conducting loop. The relevant results find application in the interference analysis of a device, equipment or system in relation to their ElectroMagnetic Compatibility (EMC) (see Chapter 30). Note that the volume source electric currents give no contribution to the magnetic near field, while the volume source magnetic currents give no contribution to the electric near field.

Exercises

Exercise 26.3-1

Employ three-dimensional spatial Fourier-transformation methods to construct the solution of the electromagnetic vector Helmholtz equation

$$\varepsilon_{k,m,p} \partial_m (\varepsilon_{p,n,r} \partial_n \hat{F}_r) + \hat{\gamma}^2 \hat{F}_k = \hat{Q}_k \tag{26.3-17}$$

that shows an exponential decay as $|x| \to \infty$ when $\mathrm{Re}(s) > 0$. In Equation (26.3-17), $\hat{\gamma} = (\hat{\eta}\hat{\zeta})^{1/2}$, and $\hat{Q}_k$ differs from zero in a bounded subdomain $\mathcal{D}^T$ of $\mathcal{R}^3$ only.

(a) Determine the equation that results upon Fourier transforming Equation (26.3-17) according to

$$\tilde{F}_k(\mathrm{j}k,s) = \int_{x \in \mathcal{R}^3} \exp(\mathrm{j}k_s x_s) \hat{F}(x,s) \, \mathrm{d}V. \tag{26.3-18}$$

(b) Rewrite the result by using the identity $\varepsilon_{k,m,p}\varepsilon_{p,n,r} = \delta_{k,n}\delta_{m,r} - \delta_{k,r}\delta_{m,n}$.

(c) Derive an expression for $k_r \tilde{F}_k$ from the resulting equation.

(d) Use the expression obtained under (c) to solve for $\tilde{F}_k$.
(e) Transform the expression for $\tilde{F}_k$ back to the complex frequency-domain configuration space.
(f) Write the result as

$$\hat{F}_k(x,s) = \int_{x' \in \mathcal{D}^\tau} \hat{G}_{k,r}(x-x',s)\hat{Q}_r(x',s)\,\mathrm{d}V \tag{26.3-19}$$

and determine $\hat{G}_{k,r}$.

Answers:

(a) $-\varepsilon_{k,m,p}\varepsilon_{p,n,r}k_m k_n \tilde{F}_r + \hat{\gamma}^2\tilde{F}_k = \tilde{Q}_k$;

(b) $-k_k k_r \tilde{F}_r + k_m k_m \tilde{F}_k + \hat{\gamma}^2\tilde{F}_k = \tilde{Q}_k$;

(c) $k_r\tilde{F}_r = \hat{\gamma}^{-2}k_r\tilde{Q}_r$;

(d) $\tilde{F}_k = \tilde{G}[\tilde{Q}_k + \hat{\gamma}^{-2}k_k k_r\tilde{Q}_r]$, with $\tilde{G} = (k_m k_m + \hat{\gamma}^2)^{-1}$;

(e) See Equation (26.3-19), with

(f) $\hat{G}_{k,r} = (\delta_{k,r} - \hat{\gamma}^{-2}\partial_k\partial_r)\hat{G}$, (26.3-20)

in which $\hat{G}(x,s) = \exp(-\hat{\gamma}|x|)/4\pi|x|$ for $|x| \neq 0$.

26.4 The time-domain source-type representations for the electric and the magnetic field strengths in a lossless medium

In this section we investigate the case where the homogeneous, isotropic medium in which the sources radiate, is, in addition, lossless. Then we have $\hat{\sigma} = 0$, $\hat{\varepsilon} = \varepsilon$ and $\hat{\mu} = \mu$ where ε and μ are real positive constants independent of s. Consequently,

$$\hat{\eta} = s\varepsilon\,, \tag{26.4-1}$$

$$\hat{\xi} = s\mu\,, \tag{26.4-2}$$

and

$$\hat{\gamma} = s/c\,, \tag{26.4-3}$$

where

$$c = (\varepsilon\mu)^{-1/2}\,. \tag{26.4-4}$$

In view of Equation (26.4-3) we now have

$$\hat{G}(x,s) = \exp(-s|x|/c)/4\pi|x| \qquad \text{for } |x| \neq 0\,. \tag{26.4-5}$$

Owing to the simple way in which the Laplace-transform parameter s occurs in the complex frequency-domain field expressions, the latter's inversion back to the time domain can now be carried out with the aid of some elementary rules. The time-domain equivalents of Equations (26.3-1) and (26.3-2) contain the time-differentiated and the time-integrated forms of the source vector potentials. For the latter we employ the notation

$$\{\mathrm{I}_t\Phi_k^J, \mathrm{I}_t\Phi_j^K\}(x,t) = \left\{ \int_{t'=t_0}^{t} \Phi_k^J(x,t')\,\mathrm{d}t', \int_{t'=t_0}^{t} \Phi_j^K(x,t')\,\mathrm{d}t' \right\}, \tag{26.4-6}$$

where t_0 is the instant at which the sources have been switched on. Equation (B.1-19) and Equations (26.3-1) and (26.3-2) lead to

$$-\mu\partial_t\Phi_k^J + \varepsilon^{-1}\partial_k\partial_r \mathrm{I}_t\Phi_r^J - \varepsilon_{k,m,p}\partial_m\Phi_p^K = \chi_{\mathcal{T}}(t)E_k(x,t) \tag{26.4-7}$$

and

$$-\varepsilon\partial_t\Phi_j^K + \mu^{-1}\partial_j\partial_p \mathrm{I}_t\Phi_p^K + \varepsilon_{j,n,r}\partial_n\Phi_r^J = \chi_{\mathcal{T}}(t)H_j(x,t)\,, \tag{26.4-8}$$

respectively. Here, $\chi_{\mathcal{T}}(t) = \{0,½,1\}$ for $t\in\{\mathcal{T},\partial\mathcal{T},\mathcal{T}'\}$ is the characteristic function of the time interval $\mathcal{T} = \{t\in\mathcal{R};\ t > t_0\}$. Since the results only differ from zero in the time interval that succeeds the instant at which the sources have been switched on, Equations (26.4-7) and (26.4-8) satisfy the condition of causality. Furthermore, using the rule that the product of two functions in the complex frequency domain corresponds to a convolution in the time domain, the time-domain equivalents of Equations (26.3-3) and (26.3-4) follow as

$$\Phi_k^J(x,t) = \int_{t'\in\mathcal{T}} \mathrm{d}t' \int_{x'\in\mathcal{D}^T} G(x-x',t-t')J_k(x',t')\,\mathrm{d}V \tag{26.4-9}$$

and

$$\Phi_j^K(x,t) = \int_{t'\in\mathcal{T}} \mathrm{d}t' \int_{x'\in\mathcal{D}^T} G(x-x',t-t')K_j(x',t')\,\mathrm{d}V\,, \tag{26.4-10}$$

respectively, in which, by inversion of Equation (26.4-5),

$$G(x,t) = \delta(t-|x|/c)/4\pi|x| \qquad \text{for } |x| \neq 0\,. \tag{26.4-11}$$

In view of the sifting property of the Dirac delta function in Equation (26.4-11), Equations (26.4-9) and (26.4-10) can be rewritten as

$$\Phi_k^J(x,t) = \int_{x'\in\mathcal{D}^T} \frac{J_k(x',t-|x-x'|/c)}{4\pi|x-x'|}\,\mathrm{d}V \tag{26.4-12}$$

and

$$\Phi_j^K(x,t) = \int_{x'\in\mathcal{D}^T} \frac{K_j(x',t-|x-x'|/c)}{4\pi|x-x'|}\,\mathrm{d}V\,, \tag{26.4-13}$$

respectively. Expressions of the type of Equations (26.4-12) and (26.4-13) are known as *retarded potentials*: the time argument in the integrands over the spatial supports of the source distributions is delayed by the travel time $|x-x'|/c$ that the electromagnetic wave needs to traverse the distance from the source point x' to the observation point x with the speed c. From this, it follows that c is the speed (*electromagnetic wave speed*) by which electromagnetic disturbances travel from the point where they originate to the point where they are observed (Figure 26.4-1). In the simple medium under consideration this wave speed is expressed in the constitutive parameters through Equation (26.4-4). In vacuum this wave speed is c_0 = 299792458 m/s (exactly).

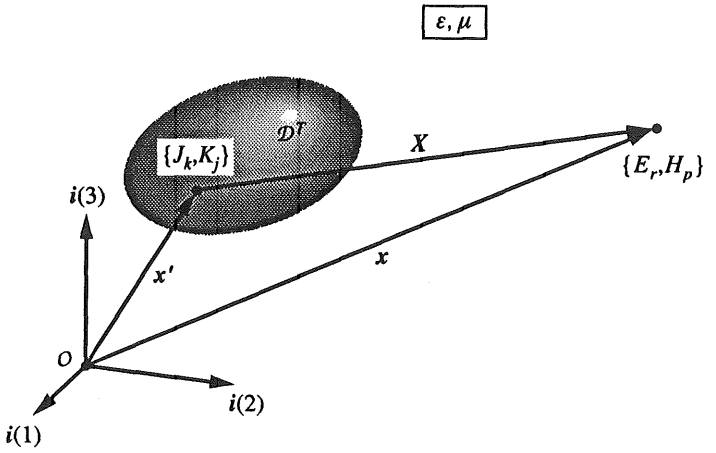

Figure 26.4-1 Time-domain source-type integral representations for the electromagnetic field $\{E_r,H_p\}$ observed at position $x\in\mathcal{R}^3$, radiated by sources $\{J_k,K_j\}$ at position $x\in\mathcal{D}^T$ (bounded source domain) in an unbounded homogeneous, isotropic, lossless medium with electromagnetic constitutive parameters $\{\varepsilon,\mu\}$ and wavespeed $c = (\varepsilon\mu)^{-1/2}$.

As to the evaluation of the expressions occurring in Equations (26.4-7)–(26.4-10) the same remarks as in Section 26.3 apply. Here, too, it is, in case numerical evaluations are necessary, advantageous to carry out the differentiations in Equations (26.4-7) and (26.4-8) with respect to the spatial coordinates analytically. As in Section 26.3 this leads to expressions that can be arranged according to their behaviour as a function of distance between source point and observation point, and in the time domain, too, the notions of near-field, intermediate-field and far-field contributions apply. The simplest way to arrive at the relevant expressions is to use Equations (26.4-1)–(26.4-3) in the complex frequency-domain expressions that are given by Equations (26.3-11)–(26.3-16) and apply the elementary rules of the inverse time Laplace transformation that have been employed earlier in this section. Upon writing

$$E_k = E_k^{\mathrm{NF}} + E_k^{\mathrm{IF}} + E_k^{\mathrm{FF}}, \tag{26.4-14}$$

and

$$H_j = H_j^{\mathrm{NF}} + H_j^{\mathrm{IF}} + H_j^{\mathrm{FF}}, \tag{26.4-15}$$

and using again the notations

$$X = x - x' \tag{26.4-16}$$

for the position vector from a source point $x'\in\mathcal{D}^T$ to the observation point $x\in\mathcal{R}^3$ and

$$\Xi_m = X_m/|X| \qquad \text{for } |X| \neq 0 \tag{26.4-17}$$

for the unit vector along X_m, we obtain in this way

$$E_k^{\mathrm{NF}}(x,t) = \varepsilon^{-1}\int_{x'\in\mathcal{D}^T}(3\Xi_k\Xi_r - \delta_{k,r})\frac{\mathrm{I}_t J_r(x',t-|X|/c)}{4\pi|X|^3}\mathrm{d}V, \tag{26.4-18}$$

$$E_k^{\mathrm{IF}}(x,t) = (\varepsilon c)^{-1}\int_{x'\in\mathcal{D}^T}(3\Xi_k\Xi_r - \delta_{k,r})\frac{J_r(x',t-|X|/c)}{4\pi|X|^2}\mathrm{d}V$$

$$+\varepsilon_{k,m,p}\int_{x'\in\mathcal{D}^T}\Xi_m\frac{K_p(x',t-|X|/c)}{4\pi|X|^2}\mathrm{d}V, \tag{26.4-19}$$

$$E_k^{\mathrm{FF}}(x,t)=\mu\int_{x'\in\mathcal{D}^T}(\Xi_k\Xi_r-\delta_{k,r})\frac{\partial_t J_r(x',t-|X|/c)}{4\pi|X|}\mathrm{d}V$$

$$+c^{-1}\varepsilon_{k,m,p}\int_{x'\in\mathcal{D}^T}\Xi_m\frac{\partial_t K_p^{\mathrm{T}}(x',t-|X|/c)}{4\pi|X|}\mathrm{d}V, \tag{26.4-20}$$

and

$$H_j^{\mathrm{NF}}(x,t)=\mu^{-1}\int_{x'\in\mathcal{D}^T}(3\Xi_j\Xi_p-\delta_{j,p})\frac{\mathrm{I}_t K_p(x',t-|X|/c)}{4\pi|X|^3}\mathrm{d}V, \tag{26.4-21}$$

$$H_j^{\mathrm{IF}}(x,t)=(\mu c)^{-1}\int_{x'\in\mathcal{D}^T}(3\Xi_j\Xi_p-\delta_{j,p})\frac{K_p(x',t-|X|/c)}{4\pi|X|^2}\mathrm{d}V$$

$$-\varepsilon_{j,n,r}\int_{x'\in\mathcal{D}^T}\Xi_n\frac{J_r(x',t-|X|/c)}{4\pi|X|^2}\mathrm{d}V, \tag{26.4-22}$$

$$H_j^{\mathrm{FF}}(x,t)=\varepsilon\int_{x'\in\mathcal{D}^T}(\Xi_j\Xi_p-\delta_{j,p})\frac{\partial_t K_p(x',t-|X|/c)}{4\pi|X|}\mathrm{d}V$$

$$-c^{-1}\varepsilon_{j,n,r}\int_{x'\in\mathcal{D}^T}\Xi_n\frac{\partial_t J_r^{\mathrm{T}}(x',t-|X|/c)}{4\pi|X|}\mathrm{d}V. \tag{26.4-23}$$

Note that in the near-field expressions the time-integrated pulse shapes of the source current densities occur, in the intermediate-field expressions the pulse shapes of the source current densities themselves, and in the far-field expressions their time-differentiated pulse shapes.

Exercises

Exercise 26.4-1

The problem of Exercise 26.3-1 is reconsidered for the case where $\hat{\gamma} = s/c$. Determine the time-domain result that follows from Equations (26.3-19) and (26.3-20).

Answer:

$$F_k(x,t)=\int_{x'\in\mathcal{D}^T}\frac{Q_k(x',t-|x-x'|/c)}{4\pi|x-x'|}\mathrm{d}V$$

$$-c^2\partial_k\partial_r\int_{x'\in\mathcal{D}^T}\frac{\mathrm{I}_t^2 Q_k(x',t-|x-x'|/c)}{4\pi|x-x'|}\mathrm{d}V, \tag{26.4-24}$$

where $\mathrm{I}_t^2 Q_k$ is the twice time-integrated pulse shape of Q_k.

26.5 The Green's function of the dissipative scalar wave equation

The wave equation that corresponds to the complex frequency-domain scalar Helmholtz equation (see Equation (26.2-4))

$$(\partial_m \partial_m - \hat{\gamma}^2)\hat{G} = -\delta(x)\,, \tag{26.5-1}$$

with

$$\hat{\gamma} = c^{-1}\,[(s+\alpha)(s+\beta)]^{1/2}\,, \tag{26.5-2}$$

in which c is a real, positive constant and α and β are real, non-negative constants, will be denoted as the dissipative scalar wave equation for point-source excitation. It obviously applies to a medium with conductive electric and linear hysteresis magnetic losses (for which case $\alpha = \sigma/\varepsilon$, $\beta = \Gamma/\mu$, $c = (\varepsilon\mu)^{-1/2}$), but also occurs in other branches of mathematical physics. With the aid of some standard rules of the time Laplace transformation the time-domain equivalent of Equation (26.5-1), i.e. the *dissipative wave equation* with point-source excitation, is found as

$$\partial_m \partial_m G - c^{-2}(\partial_t + \alpha)(\partial_t + \beta)G = -\delta(x,t)\,, \tag{26.5-3}$$

or

$$\partial_m \partial_m G - c^{-2}\partial_t^2 G - [(\alpha+\beta)/c^2]\,\partial_t G - (\alpha\beta/c^2)G = -\delta(x,t)\,. \tag{26.5-4}$$

The solution $G = G(x,t)$ of this equation is denoted as the *Green's function of the dissipative wave equation*. The ranges of the parameter values in the dissipative wave equation are: $0 < c < \infty$, $\alpha \leqslant 0 < \infty$, $\beta \leqslant 0 < \infty$. From the results it will be clear that c is the *wave speed*; α and β are denoted as *relaxation parameters*.

The solution of Equation (26.5-1) is still given by (see Equation (26.2-10))

$$\hat{G} = \exp(-\hat{\gamma}|x|)/4\pi|x| \qquad \text{for } |x| \neq 0\,. \tag{26.5-5}$$

The time-domain equivalent $G = G(x,t)$ of $\hat{G} = \hat{G}(x,s)$ as given by Equation (26.5-5) will be determined by first determining the time-domain equivalent of the function

$$\hat{U}_0 = \hat{U}_0(\alpha,\beta,T,s) = \frac{\exp(-\hat{\gamma}cT)}{\hat{\gamma}c} = \frac{\exp\{-[(s+\alpha)(s+\beta)]^{1/2}T\}}{[(s+\alpha)(s+\beta)]^{1/2}}\,. \tag{26.5-6}$$

The latter is done by evaluating the Bromwich inversion integral

$$U_0(\alpha,\beta,T,t) = \frac{1}{2\pi \mathrm{j}} \int_{s\in \mathrm{Br}} \exp(st)\hat{U}_0(\alpha,\beta,T,s)\,\mathrm{d}s\,, \tag{26.5-7}$$

where $\mathrm{Br} = \{s \in C;\ \mathrm{Re}(s) = s_0\}$ is the Bromwich path, in which, in view of the condition of causality, s_0 is chosen so large that $\hat{U}_0$ is analytic in the half-plane $\{s \in C;\ \mathrm{Re}(s) > s_0\}$ to the right of Br. As we will evaluate the integral on the right-hand side of Equation (26.5-7) by closing the contour to the left, it is necessary to identify the singularities of the integrand in the half-plane $\{s \in C;\ \mathrm{Re}(s) < s_0\}$ to the left of Br. As such we encounter the branch points $s = -\alpha$ and $s = -\beta$ on the negative real s axis, which are associated with the square-root expression. The corresponding branch cuts are chosen such that $\mathrm{Re}(s+\alpha)^{1/2} \geqslant 0$ and $\mathrm{Re}(s+\beta)^{1/2} \geqslant 0$ for all

$s \in C$, i.e. they run along $\{s \in C;\ -\infty < \mathrm{Re}(s) < -\alpha,\ \mathrm{Im}(s) = 0\}$ and $\{s \in C;\ -\infty < \mathrm{Re}(s) < -\beta,\ \mathrm{Im}(s) = 0\}$, respectively, i.e. along the negative real s axis from the pertaining branch points to infinity (Figure 26.5-1). For the product $[(s+\alpha)(s+\beta)]^{1/2}$ this implies that only a branch cut remains along $\{s \in C;\ -\max(\alpha,\beta) < \mathrm{Re}(s) < -\min(\alpha,\beta), \mathrm{Im}(s) = 0\}$, i.e. along the finite portion of the negative real s axis between the two branch points. In accordance with this choice of the branch cuts we have the asymptotic relationship

$$[(s+\alpha)(s+\beta)]^{1/2} = s + O(1) \qquad \text{as } |s| \to \infty\,, \tag{26.5-8}$$

uniformly in $\arg(s)$. On account of this relation, Jordan's lemma can be used to supplement the Bromwich contour with a semi-circle to the right for $t < T$ and with a semi-circle to the left for $t > T$. (The contribution from both semi-circles then vanishes in the limit $|s| \to \infty$.) Now, in view of Cauchy's theorem, the integration along the resulting closed contour yields the value zero for $t < T$, while for $t > T$ the resulting integral is replaced by the one that is contracted along the branch cut (Figure 26.5-2).

In the latter integral, the variable of integration s is replaced by ψ according to

$$s = -(\alpha+\beta)/2 + (|\beta-\alpha|/2)\cos(\psi) \qquad \text{with } 0 \leq \psi < 2\pi\,, \tag{26.5-9}$$

through which

$$\mathrm{d}s = -(|\beta-\alpha|/2)\sin(\psi)\,\mathrm{d}\psi \tag{26.5-10}$$

and, with the given definition of the square root,

$$[(s+\alpha)(s+\beta)]^{1/2} = \mathrm{j}(|\beta-\alpha|/2)\sin(\psi)\,. \tag{26.5-11}$$

Using this in Equations (26.5-6) and (26.5-7), we arrive at

$$U_0(\alpha,\beta,T,t) = \exp\{-[(\alpha+\beta)/2]t\}$$
$$\frac{1}{2\pi}\int_{\psi=0}^{2\pi} \exp\{(|\beta-\alpha|/2)\,[t\cos(\psi) - \mathrm{j}T\sin(\psi)]\}\,\mathrm{d}\psi \qquad \text{for } t > T\,. \tag{26.5-12}$$

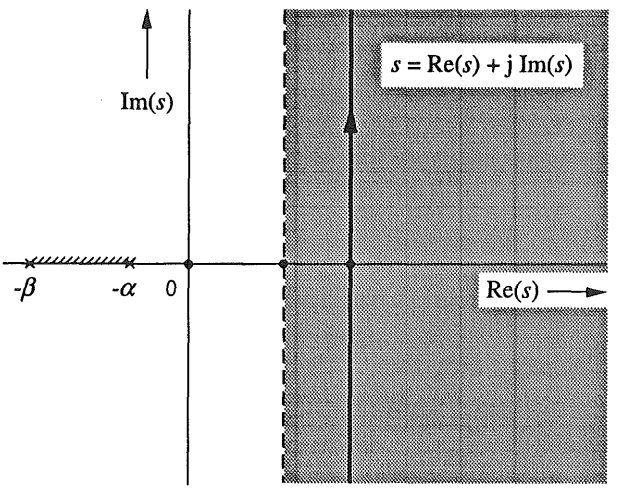

Figure 26.5-1 Bromwich contour in the complex s plane, and branch cuts, for the evaluation of the Green's function of the dissipative wave equation with relaxation parameters α and β.

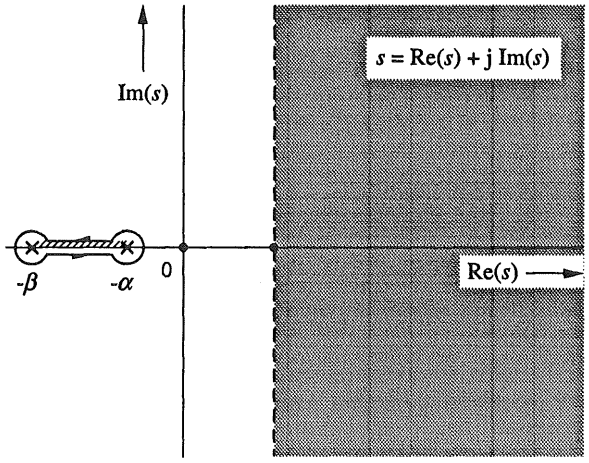

Figure 26.5-2 Contour around the branch cut of $[(s+\alpha)(s+\beta)]^{1/2}$ for the evaluation of the Green's function of the dissipative wave equation with relaxations parameters α and β.

To reduce the integral on the right-hand side to a recognizable form, we introduce the parameter τ through

$$\cosh(\tau) = \frac{t}{(t^2 - T^2)^{1/2}} \qquad \text{for } T<t<\infty\,, \tag{26.5-13}$$

which relation maps the interval $T<t<\infty$ onto $0<\tau<\infty$. Equation (26.5-13) implies that

$$\sinh(\tau) = \frac{T}{(t^2 - T^2)^{1/2}} \qquad \text{for } T<t<\infty\,, \tag{26.5-14}$$

and, hence,

$$t\cos(\psi) - jT\sin(\psi) = (t^2 - T^2)^{1/2}\cos(\psi + j\tau)\,. \tag{26.5-15}$$

The resulting integrand is continued analytically into the complex ψ plane away from the real interval $0\leqslant\psi<2\pi$ during which continuation it remains analytic and periodic in ψ with period 2π. Upon introducing

$$X = (|\beta - \alpha|/2)(t^2 - T^2)^{1/2} \qquad \text{for } T<t<\infty\,, \tag{26.5-16}$$

next shifting the path of integration from $\psi = 0$ to $\psi = 2\pi$, to $\psi = -j\tau$ to $\psi = -j\tau + 2\pi$, which is permitted in view of the periodicity of the integrand and Cauchy's theorem, and subsequently putting $\psi = -j\tau + \theta$ with $0\leqslant\theta<2\pi$, we have

$$\frac{1}{2\pi}\int_{\psi=0}^{2\pi} \exp[X\cos(\psi + j\tau)]\,d\psi = \frac{1}{2\pi}\int_{\theta=0}^{2\pi} \exp[X\cos(\theta)]\,d\theta = I_0(X)\,, \tag{26.5-17}$$

where I_0 is the modified Bessel function of the first kind and order zero (see, Abramowitz and Stegun 1964a). Collecting the results, we end up with

$$U_0(\alpha,\beta,T,t) = \exp\{-[(\alpha+\beta)/2]t\} I_0\left[(|\beta-\alpha|/2)(t^2-T^2)^{1/2}\right] H(t-T)\,, \tag{26.5-18}$$

where H denotes the Heaviside unit step function. Figure 26.5-3 shows U_0 as a function of t/T for different values of αT and βT. Since $I_0(0) = 1$, the initial value $U_0(\alpha,\beta,T,t)$ of U_0 is found to be

$$U_0(\alpha,\beta,T,t) = \exp\{-[(\alpha+\beta)/2]T\}\,, \tag{26.5-19}$$

while asymptotically

$$U_0(\alpha,\beta,T,t) \sim [2\pi(|\beta-\alpha|/2)t]^{-1/2} \exp[-\min(\alpha,\beta)t] \qquad \text{as } t\to\infty\,. \tag{26.5-20}$$

When $\beta = \alpha$, as $I_0(0) = 1$ we have

$$U_0(\alpha,\alpha,T,t) = \exp(-\alpha t)H(t-T)\,. \tag{26.5-21}$$

Now that U_0 has been determined, we return to the evaluation of G, for which $\hat{G}$ is given by Equation (26.5-5). To this end, we first observe that

$$\hat{\gamma}|x| = [(s+\alpha)(s+\beta)]^{1/2}|x|/c\,. \tag{26.5-22}$$

Now, differentiation of Equation (26.5-6) with respect to T yields

$$-\partial_T \hat{U}_0(\alpha,\beta,T,s) = \exp\{-[(s+\alpha)(s+\beta)]^{1/2}T\} \tag{26.5-23}$$

and, hence,

$$\exp(-\hat{\gamma}|x|) = [-\partial_T \hat{U}_0(\alpha,\beta,T,s)]_{T=|x|/c}\,. \tag{26.5-24}$$

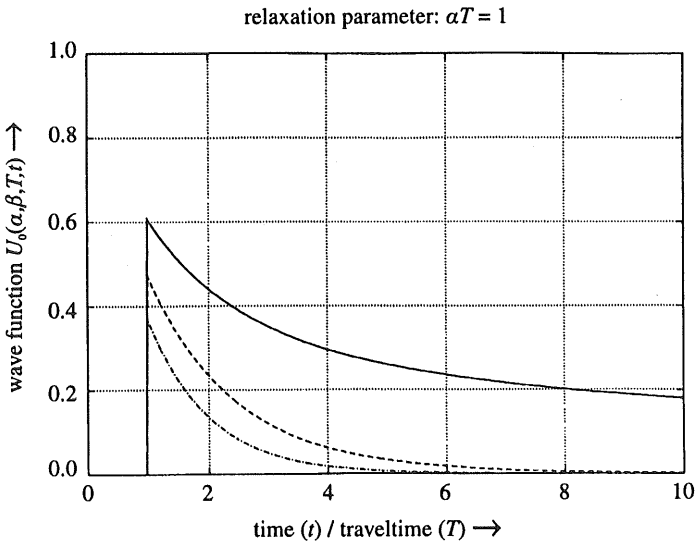

Figure 26.5-3 The wave function $U_0 = U_0(\alpha,\beta,T,t)$ as a function of normalised time t/T, with αT and βT as normalised relaxation parameters. (——): $\alpha T = 1.0$, $\beta T = 0.0$; (- - -): $\alpha T = 1.0$, $\beta T = 0.5$; (-·-·-): $\alpha T = 1.0$, $\beta T = 1.0$.

Upon introducing

$$\hat{U}_1(\alpha,\beta,T,s) = -\partial_T \hat{U}_0(\alpha,\beta,T,s) = \hat{\gamma} c \hat{U}_0(\alpha,\beta,T,s) \tag{26.5-25}$$

and, correspondingly,

$$U_1(\alpha,\beta,T,t) = -\partial_T U_0(\alpha,\beta,T,t)\,, \tag{26.5-26}$$

the expression for $\hat{G}$ can be written as

$$\hat{G} = \frac{\hat{U}_1(\alpha,\beta,|x|/c,s)}{4\pi|x|} \qquad \text{for } |x| \neq 0\,. \tag{26.5-27}$$

Hence,

$$G = \frac{U_1(\alpha,\beta,|x|/c,t)}{4\pi|x|} \qquad \text{for } |x| \neq 0\,. \tag{26.5-28}$$

Carrying out the differentiation with respect to T in Equation (26.5-18), U_1 is found as

$$U_1(\alpha,\beta,T,t) = \exp\{-[(\alpha+\beta)/2]T\}\delta(t-T) + \exp\{-[(\alpha+\beta)/2]t\} \frac{(|\beta-\alpha|/2)T}{(t^2-T^2)^{1/2}} I_1[(|\beta-\alpha|/2)(t^2-T^2)^{1/2}]H(t-T)\,, \tag{26.5-29}$$

in which $\delta(t-T)$ is the Dirac distribution operative at $t = T$, and

$$I_1(X) = \partial_X I_0(X) \tag{26.5-30}$$

is the modified Bessel function of the first kind and order one (see, Abramowitz and Stegun 1964b).

For the special case $\beta = \alpha$ we have

$$U_1(\alpha,\alpha,T,t) = \exp(-\alpha T)\delta(t-T)\,. \tag{26.5-31}$$

As compared with the lossless case, for which

$$G = \frac{U_1(0,0,|x|/c,t)}{4\pi|x|} = \frac{\delta(t-|x|/c)}{4\pi|x|} \qquad \text{for } |x| \neq 0\,, \tag{26.5-32}$$

the first term on the right-hand side of Equation (26.5-29) is an attenuated delta pulse to the attenuation of which both relaxation parameters α and β contribute in an equal manner, while the second term represents a tail that is absent in the lossless case and that yields an asymptotic contribution

$$U_1(\alpha,\beta,T,t) \sim (|\beta-\alpha|T/2)[2\pi(|\beta-\alpha|/2)t^3]^{-1/2} \exp[-\min(\alpha,\beta)t] \qquad \text{as } t\to\infty\,, \tag{26.5-33}$$

to the asymptotic decay of which only $\min(\alpha,\beta)$, i.e. the smaller of the two relaxation parameters, contributes and which has an amplitude decay proportional to $t^{-3/2}$.

The results of this section will be used to determine the time-domain source-type integral representations for the electric and the magnetic field strengths in a medium with conductive electric and linear hysteresis magnetic losses. In the relevant expressions we also need the first-and second-order spatial derivatives of $G = G(\alpha,\beta,|x|/c,t)$, and hence of $U_1 = U_1(\alpha,\beta,|x|/c,t)$. For the derivatives of the latter, denoting $|x|/c$ by T, we employ the notation

$$U_2(\alpha,\beta,T,t) = -\partial_T U_1(\alpha,\beta,T,t) \tag{26.5-34}$$

and

$$U_3(\alpha,\beta,T,t) = -\partial_T U_2(\alpha,\beta,T,t)\,. \tag{26.5-35}$$

Although these derivatives can be expressed in terms of higher-order modified Bessel functions of the first kind, the expressions become somewhat complicated, while they are probably not the most efficient ones for their numerical evaluation. As far as the latter aspect is concerned, the integral representation Equation (26.5-12) that we started with seems a more promising point of departure. This will be briefly discussed at the end of this section.

By straightforward differentiation of Equation (26.5-27) the spatial derivatives of G needed in our further analysis are obtained as

$$\partial_m G(\boldsymbol{x},t) = \frac{1}{4\pi}\left(-\frac{U_1}{|\boldsymbol{x}|^2} - \frac{U_2}{c|\boldsymbol{x}|}\right)\frac{x_m}{|\boldsymbol{x}|} \qquad \text{for } |\boldsymbol{x}| \neq 0 \tag{26.5-36}$$

and

$$\begin{aligned}\partial_r\partial_k G(\boldsymbol{x},t) = \frac{1}{4\pi}\Bigg[&\frac{U_1}{|\boldsymbol{x}|^3}\left(\frac{3x_r x_k}{|\boldsymbol{x}|^2} - \delta_{r,k}\right)\\ &+ \frac{U_2}{c|\boldsymbol{x}|^2}\left(\frac{3x_r x_k}{|\boldsymbol{x}|^2} - \delta_{r,k}\right) + \frac{U_3}{c^2|\boldsymbol{x}|}\frac{x_r x_k}{|\boldsymbol{x}|^2}\Bigg] \qquad \text{for } |\boldsymbol{x}| \neq 0\,.\end{aligned} \tag{26.5-37}$$

These results will be used in Section 26.6.

Numerical evaluation of the Green's function and its derivatives

For the computation of the Green's function and its derivatives the integral representation Equation (26.5-12) for U_0 can profitably be taken as the point of departure. First of all, it is observed that

$$U_0(\alpha,\beta,T,t) = U_0(\beta,\alpha,T,t)\,, \tag{26.5-38}$$

so that, as far as the parameters α and β are concerned, the range of computed values can be restricted to, for example, $\beta \geqslant \alpha$. Next, we shall show that

$$U_0(\alpha,\beta,T,T) = \exp\{-[(\alpha+\beta)/2]T\}\,. \tag{26.5-39}$$

To this end, it is observed that, in view of the analyticity of the integrand in the complex ψ plane and its periodicity in ψ with period 2π, we have

$$\begin{aligned}&\frac{1}{2\pi}\int_{\psi=0}^{2\pi} \exp[(|\beta-\alpha|/2)T\exp(-\mathrm{j}\psi)]\,\mathrm{d}\psi\\ &= \lim_{\tau\to\infty}\frac{1}{2\pi}\int_{\psi=-\mathrm{j}\tau}^{-\mathrm{j}\tau+2\pi} \exp[(|\beta-\alpha|/2)T\exp(-\mathrm{j}\psi)]\,\mathrm{d}\psi\\ &= \lim_{\tau\to\infty}\frac{1}{2\pi}\int_{\psi'=0}^{2\pi} \exp[(|\beta-\alpha|/2)T\exp(-\tau-\mathrm{j}\psi')]\,\mathrm{d}\psi'\\ &= 1\,,\end{aligned} \tag{26.5-40}$$

by which Equation (26.5-38) follows. For $t > T$, Equation (26.5-12) is, by subdividing the range of integration into four parts of $\pi/2$ each, rewritten as

$$U_0(\alpha,\beta,t,T) = \frac{1}{\pi}\int_{\psi=0}^{\pi/2} \left[\exp\{-(\beta/2)t[1-\cos(\psi)] - (\alpha/2)t[1+\cos(\psi)]\}\right.$$

$$\left. + \exp\{-(\beta/2)t[1+\cos(\psi)] - (\alpha/2)t[1-\cos(\psi)]\}\right] \cos[(|\beta-\alpha|/2)T\sin(\psi)]\, d\psi \,, \quad (26.5\text{-}41)$$

in which we have taken care that all exponential functions have non-positive arguments to avoid the loss of significant figures. It is noted that Equation (26.5-41) shows the symmetry in α and β. Equation (26.5-41) is suitable for numerical evaluation with the aid of any standard integration rule (for example, the trapezoidal rule). The corresponding representations for U_1, U_2 and U_3 directly follow from Equation (26.5-41) by differentiation with respect to T (see Equations (26.5-26), (26.5-34) and (26.5-35)).

Exercises

Exercise 26.5-1

What is the complex frequency-domain equivalent of $U_2 = U_2(\alpha,\beta,T,t)$ as given by Equation (26.5-34)?

Answer:

$$\hat{U}_2(\alpha,\beta,T,s) = (\hat{\gamma}c)^2\hat{U}_0(\alpha,\beta,T,s) = \hat{\gamma}c\exp(-\hat{\gamma}cT)\,.$$

Exercise 26.5-2

What is the complex frequency-domain equivalent of $U_3 = U_3(\alpha,\beta,T,t)$ as given by Equation (26.5-35)?

Answer:

$$\hat{U}_3(\alpha,\beta,T,s) = (\hat{\gamma}c)^3\hat{U}_0(\alpha,\beta,T,s) = (\hat{\gamma}c)^2\exp(-\hat{\gamma}cT)\,.$$

26.6 Time-domain source-type integral representations for the electric and the magnetic field strengths in a medium with conductive electric and linear hysteresis magnetic losses

In this section we investigate the case where the homogeneous, isotropic medium in which the sources radiate has conductive electric and linear hysteresis magnetic losses. Then, we have

$$\hat{\eta} = (s+\alpha)\varepsilon\,, \quad (26.6\text{-}1)$$

$$\hat{\zeta} = (s+\beta)\mu\,, \quad (26.6\text{-}2)$$

$$\hat{\gamma} = [(s+\alpha)(s+\beta)]^{1/2}/c\,, \tag{26.6-3}$$

with

$$\alpha = \sigma/\varepsilon,\ \beta = \Gamma/\mu,\ c = (\varepsilon\mu)^{-1/2}\,, \tag{26.6-4}$$

in which ε, μ and c are real positive constants, and σ, Γ, α and β are real, non-negative constants. In view of Equation (26.6-3) we now have

$$\hat{G}(\boldsymbol{x},s) = \frac{\exp\{-[(s+\alpha)(s+\beta)]^{1/2}\,|\boldsymbol{x}|/c\}}{4\pi|\boldsymbol{x}|} \qquad \text{for } |\boldsymbol{x}| \neq 0\,. \tag{26.6-5}$$

With the aid of the expressions derived in Section 26.5, Equation (26.6-5) leads to the time-domain result (see Equation (26.5-28))

$$G(\boldsymbol{x},t) = \frac{U_1(\alpha,\beta,|\boldsymbol{x}|/c,t)}{4\pi|\boldsymbol{x}|} \qquad \text{for } |\boldsymbol{x}| \neq 0\,, \tag{26.6-6}$$

in which U_1 is given by Equation (26.5-29). Applying standard rules of the time Laplace transformation, the time-domain expressions for the electric and the magnetic field strengths are obtained from Equations (26.3-1)–(26.3-6). In the result we use the property that the factor $s + \alpha$ corresponds to the operation $\partial_t + \alpha$ and the factor $(s + \alpha)^{-1}$ corresponds to the operation of time convolution with the function $\exp(-\alpha t)H(t)$. For these operations we employ the notation

$$\partial_t^{\alpha}\{J_r,K_p\}(\boldsymbol{x},t) = (\partial_t + \alpha)\{J_r,K_p\}(\boldsymbol{x},t) \tag{26.6-7}$$

and

$$\mathrm{I}_t^{\alpha}\{J_r,K_p\}(\boldsymbol{x},t) = \left[\int_{t'=0}^{\infty} \exp(-\alpha t')\{J_r,K_p\}(\boldsymbol{x},t-t')\,\mathrm{d}t'\right] H(t)\,. \tag{26.6-8}$$

With this, we obtain (see Equations (26.3-1) and (26.3-2))

$$-\mu\partial_t^{\beta}\Phi_k^J + \varepsilon^{-1}\mathrm{I}_t^{\alpha}\partial_k\partial_r\Phi_r^J - \varepsilon_{k,m,p}\partial_m\Phi_p^K = \chi_{\mathcal{T}}(t)E_k(\boldsymbol{x},t) \tag{26.6-9}$$

and

$$-\varepsilon\partial_t\Phi_j^K + \mu^{-1}\mathrm{I}_t^{\beta}\partial_j\partial_p\Phi_p^K + \varepsilon_{j,n,r}\partial_n\Phi_p^J = \chi_{\mathcal{T}}(t)H_j(\boldsymbol{x},t)\,, \tag{26.6-10}$$

in which (see Equations (26.3-3) and (26.3-4))

$$\Phi_k^J(\boldsymbol{x},t) = \int_{t'\in\mathcal{T}} \mathrm{d}t' \int_{\boldsymbol{x}'\in\mathcal{D}^T} G(\boldsymbol{x}-\boldsymbol{x}',t-t')J_k(\boldsymbol{x}',t')\mathrm{d}V \tag{26.6-11}$$

and

$$\Phi_j^K(\boldsymbol{x},t) = \int_{t'\in\mathcal{T}} \mathrm{d}t' \int_{\boldsymbol{x}'\in\mathcal{D}^T} G(\boldsymbol{x}-\boldsymbol{x}',t-t')K_j(\boldsymbol{x}',t')\mathrm{d}V\,. \tag{26.6-12}$$

As to the evaluation of the expressions occurring in Equations (26.6-9)–(26.6-12), the same remarks as in Section 26.4 apply. Here, too, it is, in case numerical evaluations are necessary, advantageous to carry out the differentiations with respect to the spatial coordinates analytically. This again leads to expressions that can be arranged according to their behaviour as a function

of the distance from the source point to an observation point, and in the present case as well, the notions of near-field, intermediate-field and far-field contributions apply. The easiest way to arrive at the pertaining expressions is to transform Equations (26.3-9)–(26.3-12) back to the time domain with the aid of the results of Section 26.5. Again writing

$$E_k = E_k^{\mathrm{NF}} + E_k^{\mathrm{IF}} + E_k^{\mathrm{FF}} \tag{26.6-13}$$

and

$$H_j = H_j^{\mathrm{NF}} + H_j^{\mathrm{IF}} + H_j^{\mathrm{FF}}, \tag{26.6-14}$$

this procedure leads to

$$E_k^{\mathrm{NF}}(x,t) = \varepsilon^{-1}\mathrm{I}_t^{\alpha}\int_{t'\in\mathcal{T}}\mathrm{d}t'\int_{x'\in\mathcal{D}^T}(3\Xi_k\Xi_r-\delta_{k,r})J_r(x',t')\frac{U_1(\alpha,\beta,|x|/c,t-t')}{4\pi|X|^3}\mathrm{d}V, \tag{26.6-15}$$

$$\begin{aligned}E_k^{\mathrm{IF}}(x,t) = {}&(\varepsilon c)^{-1}\mathrm{I}_t^{\alpha}\int_{t'\in\mathcal{T}}\mathrm{d}t'\int_{x'\in\mathcal{D}^T}(3\Xi_k\Xi_r-\delta_{k,r})J_r(x',t')\frac{U_2(\alpha,\beta,|x|/c,t-t')}{4\pi|X|^2}\mathrm{d}V\\ &+\varepsilon_{k,m,p}\int_{t'\in\mathcal{T}}\mathrm{d}t'\int_{x'\in\mathcal{D}^T}\Xi_m K_p(x',t')\frac{U_1(\alpha,\beta,|x|/c,t-t')}{4\pi|X|^2}\mathrm{d}V,\end{aligned} \tag{26.6-16}$$

$$\begin{aligned}E_k^{\mathrm{FF}}(x,t) = {}&\mu\partial_t^{\beta}\int_{t'\in\mathcal{T}}\mathrm{d}t'\int_{x'\in\mathcal{D}^T}(\Xi_k\Xi_r-\delta_{k,r})J_r(x',t')\frac{U_1(\alpha,\beta,|x|/c,t-t')}{4\pi|X|}\mathrm{d}V\\ &+c^{-1}\varepsilon_{k,m,p}\int_{t'\in\mathcal{T}}\mathrm{d}t'\int_{x'\in\mathcal{D}^T}\Xi_m K_p(x',t')\frac{U_2(\alpha,\beta,|x|/c,t-t')}{4\pi|X|}\mathrm{d}V,\end{aligned} \tag{26.6-17}$$

and

$$H_j^{\mathrm{NF}}(x,t) = \mu^{-1}\mathrm{I}_t^{\beta}\int_{t'\in\mathcal{T}}\mathrm{d}t'\int_{x'\in\mathcal{D}^T}(3\Xi_j\Xi_p-\delta_{j,p})K_p(x',t')\frac{U_1(\alpha,\beta,|x|/c,t-t')}{4\pi|X|^3}\mathrm{d}V, \tag{26.6-18}$$

$$\begin{aligned}H_j^{\mathrm{IF}}(x,t) = {}&(\mu c)^{-1}\mathrm{I}_t^{\beta}\int_{t'\in\mathcal{T}}\mathrm{d}t'\int_{x'\in\mathcal{D}^T}(3\Xi_j\Xi_p-\delta_{j,p})K_p(x',t')\frac{U_2(\alpha,\beta,|x|/c,t-t')}{4\pi|X|^2}\mathrm{d}V\\ &-\varepsilon_{j,n,r}\int_{t'\in\mathcal{T}}\mathrm{d}t'\int_{x'\in\mathcal{D}^T}\Xi_n J_r(x',t')\frac{U_1(\alpha,\beta,|x|/c,t-t')}{4\pi|X|^2}\mathrm{d}V,\end{aligned} \tag{26.6-19}$$

$$\begin{aligned}H_j^{\mathrm{FF}}(x,t) = {}&\varepsilon\partial_t^{\alpha}\int_{t'\in\mathcal{T}}\mathrm{d}t'\int_{x'\in\mathcal{D}^T}(\Xi_j\Xi_p-\delta_{j,p})K_p(x',t')\frac{U_1(\alpha,\beta,|x|/c,t-t')}{4\pi|X|}\mathrm{d}V\\ &-c^{-1}\varepsilon_{j,n,r}\int_{t'\in\mathcal{T}}\mathrm{d}t'\int_{x'\in\mathcal{D}^T}\Xi_n J_r(x',t')\frac{U_2(\alpha,\beta,|x|/c,t-t')}{4\pi|X|}\mathrm{d}V.\end{aligned} \tag{26.6-20}$$

Here,

$$X = x - x' \tag{26.6-21}$$

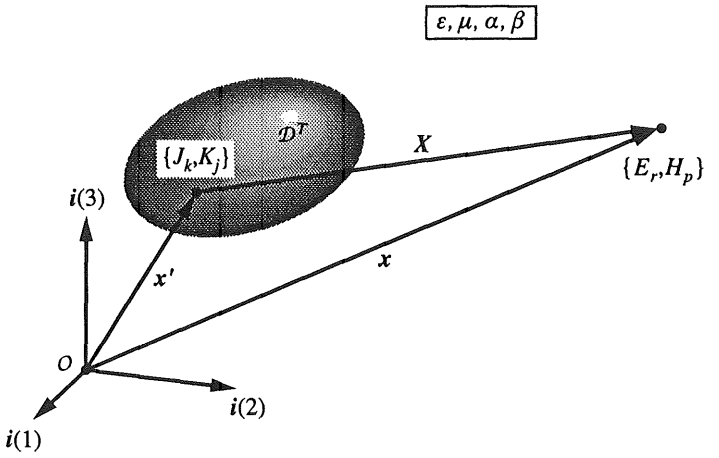

Figure 26.6-1 Time-domain source-type integral representations for the electromagnetic field $\{E_r,H_P\}$ observed at position $x\in\mathcal{R}^3$, radiated by source distributions $\{J_k,K_j\}$ at position $x\in\mathcal{D}^T$ (bounded source domain) in an unbounded, homogeneous, isotropic medium with conductive electric and linear magnetic hysteresis losses (electromagnetic constitutive parameters $\{\varepsilon,\mu,\alpha=\sigma/\varepsilon,\beta=\Gamma/\mu\}$).

is the position vector from the source point $x'\in\mathcal{D}^T$ to the observation point $x\in\mathcal{R}^3$ and

$$\Xi_m = X_m/|X| \qquad \text{for } |X|\neq 0 \tag{26.6-22}$$

is the unit vector along X_m (Figure 26.6-1).

With this the time-domain expressions for the electric and magnetic field strengths radiated by sources in a homogeneous, isotropic medium with conductive electric and linear hysteresis magnetic losses have been completed.

26.7 The Green's function of the scalar wave equation associated with plasma oscillations and superconductivity

The wave equation that corresponds to the complex frequency-domain scalar Helmholtz equation (see Equation (26.2-4))

$$(\partial_m\partial_m - \hat{\gamma}^2)\hat{G} = -\delta(x)\,, \tag{26.7-1}$$

with

$$\hat{\gamma} = c^{-1}(s^2+\omega_p^2)^{1/2}\,, \tag{26.7-2}$$

in which c is a real, positive constant (the wave speed) and ω_p is a real, non-negative constant (the plasma angular frequency), will be denoted as the wave equation associated with plasma oscillations and superconductivity, for point-source excitation. It applies to the medium that consists of a collisionless electron plasma in a vacuum background (to which category also the superconducting metal belongs). For this case, $c = c_0 = (\varepsilon_0\mu_0)^{-1/2}$ and $\omega_p = \omega_{pe}$, where ω_{pe} is the electron plasma angular frequency. With the aid of some standard rules of the time Laplace

transformation the time-domain equivalent of Equation (26.7-1), i.e. *the wave equation associated with plasma oscillations and superconductivity*, with point-source excitation, is found as

$$\partial_m\partial_m G - c^{-2}(\partial_t^{\,2} + \omega_p^{\,2})G = -\delta(x,t)\,, \tag{26.7-3}$$

or

$$\partial_m\partial_m G - c^{-2}\partial_t^{\,2}G - (\omega_p^{\,2}/c^2)G = -\delta(x,t)\,. \tag{26.7-4}$$

The solution $G = G(x,t)$ of this equation is denoted as the Green's function of the wave equation associated with plasma oscillations and superconductivity. The ranges of the parameter values in the relevant wave equation are: $0 < c < \infty$ and $0 \leqslant \omega_p < \infty$.

The solution of Equation (26.7-1) is still given by (see Equation (26.2-10))

$$\hat{G} = \exp(-\hat{\gamma}|x|)/4\pi|x| \qquad \text{for} \quad |x| \neq 0. \tag{26.7-5}$$

The time-domain equivalent $G = G(x,t)$ of $\hat{G} = \hat{G}(x,s)$ as given by Equation (26.7-5) will be determined by first determining the time-domain equivalent of the function

$$\hat{W}_0 = \hat{W}_0(\omega_p,T,s) = \frac{\exp(-\hat{\gamma}cT)}{\hat{\gamma}c} = \frac{\exp\left[-(s^2+\omega_p^2)^{1/2}T\right]}{(s^2+\omega_p^2)^{1/2}}\,. \tag{26.7-6}$$

The latter is done by evaluating the Bromwich inversion integral

$$W_0(\omega_p,T,t) = \frac{1}{2\pi j}\int_{s\in Br} \exp(st)\hat{W}_0(\omega_p,T,s)\,ds\,, \tag{26.7-7}$$

where $Br = \{s\in C;\ \mathrm{Re}(s) = s_0\}$ is the Bromwich path, in which, in view of the condition of causality, s_0 is chosen so large that $\hat{W}_0$ is analytic in the half-plane $\{s\in C;\ \mathrm{Re}(s) > s_0\}$ to the right of Br. As we shall evaluate the integral on the right-hand side of Equation (26.7-7) by closing the contour to the left, it is necessary to identify the singularities of the integrand in the half-plane $\{s\in C;\ \mathrm{Re}(s) < s_0\}$ to the left of Br. As such we encounter the branch points $s = -j\omega_p$ and $s = j\omega_p$ on the imaginary s axis, which are associated with the square-root expression. The corresponding branch cut is chosen such that $\mathrm{Re}(s^2+\omega_p^2)^{1/2} \geqslant 0$ for all $s\in C$, i.e. it runs along $\{s\in C;\ \mathrm{Re}(s) = 0, -\omega_p < \mathrm{Im}(s) < \omega_p\}$ i.e. along the imaginary s axis in between the pertaining branch points (Figure 26.7-1).

In accordance with this choice of the branch cut we have the asymptotic relationship

$$(s^2+\omega_p^{\,2})^{1/2} = s + O(s^{-1}) \qquad \text{as } |s|\to\infty\,, \tag{26.7-8}$$

uniformly in $\arg(s)$. On account of this relation, Jordan's lemma can be used to supplement the Bromwich contour with a semi-circle to the right for $t < T$ and with a semi-circle to the left for $t > T$. (The contribution from both semi-circles then vanishes in the limit $|s|\to\infty$.) Now, in view of Cauchy's theorem, the integration along the resulting closed contour yields the value zero for $t < T$ while for $t > T$ the resulting integral is replaced by the one that is contracted along the branch cut (Figure 26.7-2).

In the latter integral, the variable of integration s is replaced by ψ according to

$$s = -j\omega_p\cos(\psi) \qquad \text{with} \quad 0 \leqslant \psi < 2\pi, \tag{26.7-9}$$

through which

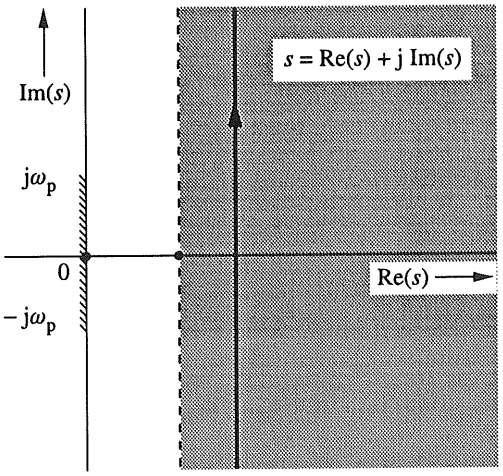

Figure 26.7-1 Bromwich contour in the complex s plane, and branch cuts, for the evaluation of the Green's function of the wave equation associated with plasma oscillations and superconductivity, with plasma angular frequency ω_p.

$$ds = j\omega_p \sin(\psi)\, d\psi\,, \tag{26.7-10}$$

and, with the given definition of the square root,

$$(s^2 + \omega_p^2)^{1/2} = \omega_p \sin(\psi)\,. \tag{26.7-11}$$

Using this in Equations (26.7-6) and (26.7-7), we arrive at

$$W_0(\omega_p, T, t) = \frac{1}{2\pi} \int_{\psi=0}^{2\pi} \exp\{-j\omega_p[t\cos(\psi) - jT\sin(\psi)]\}\, d\psi \quad \text{for} \quad t > T. \tag{26.7-12}$$

To reduce the integral on the right-hand side to a recognizable form, we introduce the parameter τ through

$$\cosh(\tau) = \frac{t}{(t^2 - T^2)^{1/2}} \qquad \text{for} \quad T < t < \infty, \tag{26.7-13}$$

which relation maps the interval $T < t < \infty$ onto $0 < \tau < \infty$. Equation (26.7-13) implies that

$$\sinh(\tau) = \frac{T}{(t^2 - T^2)^{1/2}} \qquad \text{for} \quad T < t < \infty, \tag{26.7-14}$$

and, hence,

$$t\cos(\psi) - jT\sin(\psi) = (t^2 - T^2)^{1/2}\cos(\psi + j\tau)\,. \tag{26.7-15}$$

The resulting integrand is continued analytically into the complex ψ plane away from the real interval $0 \leq \psi < 2\pi$ during which continuation it remains analytic and periodic in ψ with period 2π. Upon introducing

$$X = \omega_p(t^2 - T^2)^{1/2} \qquad \text{for} \quad T < t < \infty\,, \tag{26.7-16}$$

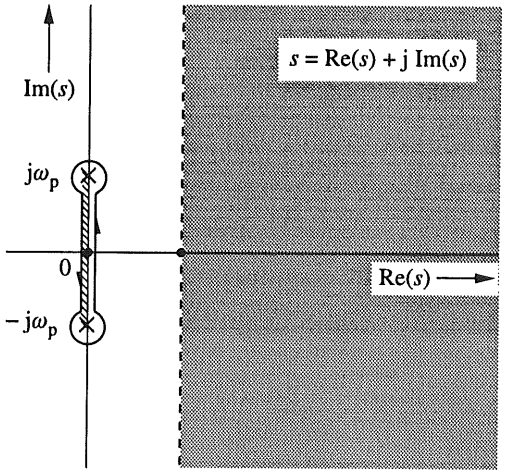

Figure 26.7-2 Contour around the branch cut of $(s^2 + \omega_p^2)^{1/2}$ for the evaluation of the Green's function of the wave equation associated with plasma oscillations and superconductivity, with plasma angular frequency ω_p.

next shifting the path of integration from $\psi = 0$ to $\psi = 2\pi$, to $\psi = -j\tau$ to $\psi = -j\tau + 2\pi$, which is permitted in view of the periodicity of the integrand and Cauchy's theorem, and subsequently putting $\psi = -j\tau + \theta$ with $0 \leqslant \theta < 2\pi$ we have

$$\frac{1}{2\pi}\int_{\psi=0}^{2\pi} \exp[-jX\cos(\psi + j\tau)]\,d\psi = \frac{1}{2\pi}\int_{\theta=0}^{2\pi} \exp[-jX\cos(\theta)]\,d\theta = J_0(X)\,, \qquad (26.7\text{-}17)$$

where J_0 is the Bessel function of the first kind and order zero (see Abramowitz and Stegun 1964c). Collecting the results, we end up with

$$W_0(\omega_p,T,t) = J_0\left[\omega_p(t^2 - T^2)^{1/2}\right]H(t - T)\,, \qquad (26.7\text{-}18)$$

where H denotes the Heaviside unit step function. Figure 26.7-3 shows W_0 as a function of t/T for different values of $\omega_p T$. Since $J_0(0) = 1$, the initial value $W_0(\omega_p,T,T)$ of W_0 is found as

$$W_0(\omega_p,T,T) = 1, \qquad (26.7\text{-}19)$$

while asymptotically

$$W_0(\omega_p,T,t) \sim (2/\pi\omega_p t)^{1/2}\cos(\omega_p t - \pi/4) \quad \text{as} \quad t \to \infty\,. \qquad (26.7\text{-}20)$$

In case $\omega_p = 0$, we have, since $J_0(0) = 1$,

$$W_0(0,T,t) = H(t - T)\,. \qquad (26.7\text{-}21)$$

Now that W_0 has been determined, we return to the evaluation of G, for which $\hat{G}$ is given by Equation (26.7-5). To this end, we first observe that

$$\hat{\gamma}|x| = (s^2 + \omega_p^2)^{1/2}|x|/c\,. \qquad (26.7\text{-}22)$$

Now, differentiation of Equation (26.7-6) with respect to T yields

$$-\partial_T \hat{W}_0(\omega_p,T,s) = \exp\left[-(s^2 + \omega_p^2)^{1/2}T\right] \qquad (26.7\text{-}23)$$

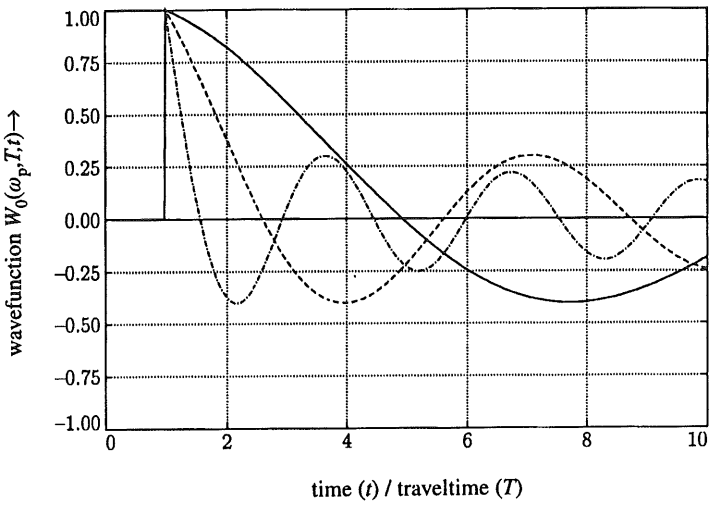

Figure 26.7-3 The wave function $W_0 = W_0(\omega_p,T,t)$ as a function of normalised time t/T, with $\omega_p T$ as normalised parameter. (——): $\omega_p T = 0.5$; (- - -): $\omega_p T = 1.0$; (-·-·-): $\omega_p T = 2.0$.

and, hence,

$$\exp(-\hat{\gamma}|x|) = [-\partial_T \hat{W}_0(\omega_p,T,s)]_{T=|x|/c} \,. \tag{26.7-24}$$

Upon introducing

$$\hat{W}_1(\omega_p,T,s) = -\partial_T \hat{W}_0(\omega_p,T,s) = \hat{\gamma} c \hat{W}_0(\omega_p,T,s) \,, \tag{26.7-25}$$

and, correspondingly,

$$W_1(\omega_p,T,t) = -\partial_T W_0(\omega_p,T,t) \,, \tag{26.7-26}$$

the expression for $\hat{G}$ can be written as

$$\hat{G} = \frac{\hat{W}_1(\omega_p,|x|/c,s)}{4\pi|x|} \quad \text{for} \quad |x| \neq 0. \tag{26.7-27}$$

Hence,

$$G = \frac{W_1(\omega_p,|x|/c,t)}{4\pi|x|} \quad \text{for} \quad |x| \neq 0. \tag{26.7-28}$$

Carrying out the differentiation with respect to T in Equation (26.7-18), W_1 is found as

$$W_1(\omega_p,T,t) = \delta(t-T) + \frac{\omega_p T}{(t^2 - T^2)^{1/2}} J_1\left[\omega_p (t^2 - T^2)^{1/2}\right] H(t-T) \,, \tag{26.7-29}$$

in which $\delta(t-T)$ is the Dirac distribution operative at $t = T$, and

$$J_1(X) = -\partial_X J_0(X) \tag{26.7-30}$$

is the Bessel function of the first kind and order one (see Abramowitz and Stegun 1964d).

For the special case $\omega_p = 0$ we have

$$W_1(0,T,t) = \delta(t - T) . \tag{26.7-31}$$

As compared with the case where no plasma is present and for which

$$G = \frac{W_1(0,|x|/c,t)}{4\pi|x|} = \frac{\delta(t - |x|/c)}{4\pi|x|} \quad \text{for} \quad |x| \neq 0 , \tag{26.7-32}$$

the first term on the right-hand side of Equation (26.7-29) yields an identical contribution, while the second term represents a tail that is characteristic for the presence of the plasma and yields an asymptotic contribution

$$W_1(\omega_p,T,t) \sim \omega_p(2/\pi\omega_p t^3)^{1/2} \sin(\omega_p t - \pi/4) \quad \text{as} \quad t \to \infty , \tag{26.7-33}$$

which contribution oscillates with the plasma angular frequency and decays in amplitude proportionally to $t^{-3/2}$ as $t \to \infty$.

The results of this section will be used to determine the time-domain source-type integral representations for the electric and the magnetic field strengths in a medium that consists of a collisionless plasma in a vacuum background (to which category also the superconducting metal belongs). In the relevant expressions we also need the first-and second-order spatial derivatives of $G = G(\omega_p,|x|/c,t)$, and hence of $W_1 = W_1(\omega_p,|x|/c,t)$. For the derivatives of the latter we shall, denoting $|x|/c$ by T, employ the notations

$$W_2(\omega_p,T,t) = -\partial_T W_1(\omega_p,T,t) \tag{26.7-34}$$

and

$$W_3(\omega_p,T,t) = -\partial_T W_2(\omega_p,T,t) . \tag{26.7-35}$$

By straightforward differentiation of Equation (26.7-27) the spatial derivatives of G needed in our further analysis are obtained as

$$\partial_m G(x,t) = \frac{1}{4\pi}\left(-\frac{W_1}{|x|^2} - \frac{W_2}{c|x|}\right)\frac{x_m}{|x|} \quad \text{for} \quad |x| \neq 0 \tag{26.7-36}$$

and

$$\partial_r\partial_k G(x,t) = \frac{1}{4\pi}\left[\frac{W_1}{|x|^3}\left(\frac{3x_r x_k}{|x|^2} - \delta_{r,k}\right)\right.$$

$$\left. + \frac{W_2}{c|x|^2}\left(\frac{3x_r x_k}{|x|^2} - \delta_{r,k}\right) + \frac{W_3}{c^2|x|}\frac{x_r x_k}{|x|^2}\right] \quad \text{for} \quad |x| \neq 0 . \tag{26.7-37}$$

These results will be used in Section 26.8.

Numerical evaluation of the Green's function and its derivatives

For the computation of the Green's function and its derivatives the integral representation for W_0 following from Equation (26.7-17) can profitably be employed, i.e.

$$W_0(\omega_p,T,t) = \left\{ \frac{1}{2\pi} \int_{\theta=0}^{2\pi} \exp\left[-j\omega_p(t^2 - T^2)^{1/2} \cos(\theta)\right] d\theta \right\} H(t-T) . \tag{26.7-38}$$

This integral can be rewritten as

$$W_0(\omega_p,T,t) = \left\{ \frac{2}{\pi} \int_{\theta=0}^{\pi/2} \cos\left[\omega_p(t^2 - T^2)^{1/2} \cos(\theta)\right] d\theta \right\} H(t-T) . \tag{26.7-39}$$

By straightforward differentiation with respect to T, the corresponding integral representations for W_1, W_2 and W_3 are obtained. The resulting integrals are suitable for numerical evaluation with the aid of any standard integration rule (for example, the trapezoidal rule). Care must be taken to incorporate the derivatives of the Heaviside unit step function in the expressions.

26.8 Time-domain source-type integral representations for the electric and the magnetic field strengths in an electron plasma or a superconducting metal

In this section we investigate the case where the homogeneous, isotropic medium in which the sources radiate is a collisionless electron plasma in a vacuum background; also the superconducting metal belongs to this category. Then, we have

$$\hat{\eta} = s\varepsilon_0(1 + \omega_{pe}^2/s^2) , \tag{26.8-1}$$

$$\hat{\zeta} = s\mu_0 , \tag{26.8-2}$$

$$\hat{\gamma} = c_0^{-1}(s^2 + \omega_{pe}^2)^{1/2} , \tag{26.8-3}$$

in which $c_0 = (\varepsilon_0\mu_0)^{-1/2}$ is a positive constant (the electromagnetic wave speed in vacuum) and ω_{pe} is a non-negative constant (the electron plasma angular frequency). In view of Equation (26.8-3) we now have

$$\hat{G}(x,s) = \frac{\exp\left[-(s^2 + \omega_{pe}^2)^{1/2}|x|/c\right]}{4\pi|x|} \quad \text{for} \quad |x| \neq 0 . \tag{26.8-5}$$

With the aid of the expressions derived in Section 26.7, Equation (26.8-5) leads to the time-domain result (see Equation (26.7-28))

$$G(x,t) = \frac{W_1(\omega_{pe},|x|/c,t)}{4\pi|x|} \quad \text{for} \quad |x| \neq 0 , \tag{26.8-6}$$

in which W_1 is given by Equation (26.7-29). Applying standard rules of the time Laplace transformation, the time-domain expressions for the electric and the magnetic field strengths are obtained from Equations (26.3-1)–(26.3-6). In the result we use the property that the factor $s + \omega_{pe}^2/s$ corresponds to the operation $\partial_t + \omega_{pe}^2 I_t$ and that the factor $(s + \omega_{pe}^2/s)^{-1}$ corresponds to the operation of time convolution with the function $\cos(\omega_{pe}t)H(t)$. For these operations we employ the notations

$$\partial_t^{\omega_{pe}}\{J_r,K_p\}(x,t) = (\partial_t + \omega_{pe}^2 I_t)\{J_r,K_p\}(x,t) , \tag{26.8-7}$$

and

$$\mathrm{I}_t^{\omega_{\mathrm{pe}}}\{J_r,K_p\}(x,t)=\int_{t'=0}^{\infty}\cos(\omega_{\mathrm{pe}}t')\{J_r,K_p\}(x,t-t')\,\mathrm{d}t'\,. \tag{26.8-8}$$

With this, we obtain

$$-\mu_0\partial_t\Phi_k^J+\varepsilon_0^{-1}\mathrm{I}_t^{\omega_{\mathrm{pe}}}\partial_k\partial_r\Phi_r^J-\varepsilon_{k,m,p}\partial_m\Phi_p^K=\chi_{\mathcal{T}}(t)E_k(x,t)\,, \tag{26.8-9}$$

and

$$-\varepsilon_0\partial_t^{\omega_{\mathrm{pe}}}\Phi_j^K+\mu_0^{-1}\mathrm{I}_t\partial_j\partial_p\Phi_p^K+\varepsilon_{j,n,r}\partial_n\Phi_r^J=\chi_{\mathcal{T}}(t)H_j(x,t)\,, \tag{26.8-10}$$

in which

$$\Phi_k^J(x,t)=\int_{t'\in\mathcal{T}}\mathrm{d}t'\int_{x'\in\mathcal{D}^T}G(x-x',t-t')J_k(x',t')\,\mathrm{d}V\,, \tag{26.8-11}$$

and

$$\Phi_j^K(x,t)=\int_{t'\in\mathcal{T}}\mathrm{d}t'\int_{x'\in\mathcal{D}^T}G(x-x',t-t')K_j(x',t')\,\mathrm{d}V\,. \tag{26.8-12}$$

As to the evaluation of the expressions occurring in Equations (26.8-9)–(26.8-12), the same remarks as in Section 26.4 apply. Here, too, it is, in case numerical evaluations are necessary, advantageous to carry out the differentiations with respect to the spatial coordinates analytically. This again leads to expressions that can be arranged according to their behaviour as a function of the distance from the source point to an observation point, and in the present case as well, the notions of near-field, intermediate-field and far-field contributions apply. Again writing

$$E_k=E_k^{\mathrm{NF}}+E_k^{\mathrm{IF}}+E_k^{\mathrm{FF}} \tag{26.8-13}$$

and

$$H_j=H_j^{\mathrm{NF}}+H_j^{\mathrm{IF}}+H_j^{\mathrm{FF}}, \tag{26.8-14}$$

this procedure leads to

$$E_k^{\mathrm{NF}}(x,t)$$

$$=\varepsilon_0^{-1}\mathrm{I}_t^{\omega_{\mathrm{pe}}}\int_{t'\in\mathcal{T}}\mathrm{d}t'\int_{x'\in\mathcal{D}^T}(3\Xi_k\Xi_r-\delta_{k,r})J_r(x',t')\,\frac{W_1(\omega_{\mathrm{pe}},|X|/c,t-t')}{4\pi|X|^3}\,\mathrm{d}V\,, \tag{26.8-15}$$

$$E_k^{\mathrm{IF}}(x,t)=(\varepsilon_0c_0)^{-1}\mathrm{I}_t^{\omega_{\mathrm{pe}}}\int_{t'\in\mathcal{T}}\mathrm{d}t'\int_{x'\in\mathcal{D}^T}(3\Xi_k\Xi_r-\delta_{k,r})J_r(x',t')\,\frac{W_2(\omega_{\mathrm{pe}},|X|/c,t-t')}{4\pi|X|^2}\,\mathrm{d}V$$

$$+\varepsilon_{k,m,p}\int_{t'\in\mathcal{T}}\mathrm{d}t'\int_{x'\in\mathcal{D}^T}\Xi_mK_p(x',t')\,\frac{W_1(\omega_{\mathrm{pe}},|X|/c,t-t')}{4\pi|X|^2}\,\mathrm{d}V\,, \tag{26.8-16}$$

$$E_k^{\mathrm{FF}}(x,t)=\mu_0\partial_t\int_{t'\in\mathcal{T}}\mathrm{d}t'\int_{x'\in\mathcal{D}^T}(\Xi_k\Xi_r-\delta_{k,r})J_r(x',t')\,\frac{W_1(\omega_{\mathrm{pe}},|X|/c,t-t')}{4\pi|X|}\,\mathrm{d}V$$

$$+c_0^{-1}\varepsilon_{k,m,p}\int_{t'\in\mathcal{T}}\mathrm{d}t'\int_{x'\in\mathcal{D}^T}\Xi_mK_p(x',t')\,\frac{W_2(\omega_{\mathrm{pe}},|X|/c,t-t')}{4\pi|X|}\,\mathrm{d}V\,, \tag{26.8-17}$$

and

$$H_j^{\mathrm{NF}}(x,t)$$

$$= \mu_0^{-1} \mathrm{I}_t \int_{t' \in \mathcal{T}} \mathrm{d}t' \int_{x' \in \mathcal{D}^T} (3\Xi_j \Xi_p - \delta_{j,p}) K_p(x',t') \frac{W_1(\omega_{\mathrm{pe}}, |X|/c, t-t')}{4\pi |X|^3} \mathrm{d}V, \tag{26.8-18}$$

$$H_j^{\mathrm{IF}}(x,t) = (\mu_0 c_0)^{-1} \mathrm{I}_t \int_{t' \in \mathcal{T}} \mathrm{d}t' \int_{x' \in \mathcal{D}^T} (3\Xi_j \Xi_p - \delta_{j,p}) K_p(x',t') \frac{W_2(\omega_{\mathrm{pe}}, |X|/c, t-t')}{4\pi |X|^2} \mathrm{d}V$$

$$- \varepsilon_{j,n,r} \int_{t' \in \mathcal{T}} \mathrm{d}t' \int_{x' \in \mathcal{D}^T} \Xi_n J_r(x',t') \frac{W_1(\omega_{\mathrm{pe}}, |X|/c, t-t')}{4\pi |X|^2} \mathrm{d}V, \tag{26.8-19}$$

$$H_j^{\mathrm{FF}}(x,t) = \varepsilon_0 \partial_t^{\omega_{\mathrm{pe}}} \int_{t' \in \mathcal{T}} \mathrm{d}t' \int_{x' \in \mathcal{D}^T} (\Xi_j \Xi_p - \delta_{j,p}) K_p(x',t') \frac{W_1(\omega_{\mathrm{pe}}, |X|/c, t-t')}{4\pi |X|} \mathrm{d}V$$

$$- c_0^{-1} \varepsilon_{j,n,r} \int_{t' \in \mathcal{T}} \mathrm{d}t' \int_{x' \in \mathcal{D}^T} \Xi_n J_r(x',t') \frac{W_2(\omega_{\mathrm{pe}}, |X|/c, t-t')}{4\pi |X|} \mathrm{d}V. \tag{26.8-20}$$

Here,

$$X = x - x' \tag{26.8-21}$$

is the position vector from the source point $x' \in \mathcal{D}^T$ to the observation point $x \in \mathcal{R}^3$ and

$$\Xi_m = X_m / |X| \qquad \text{for } |X| \neq 0, \tag{26.8-22}$$

is the unit vector along X_m (Figure 26.8-1).

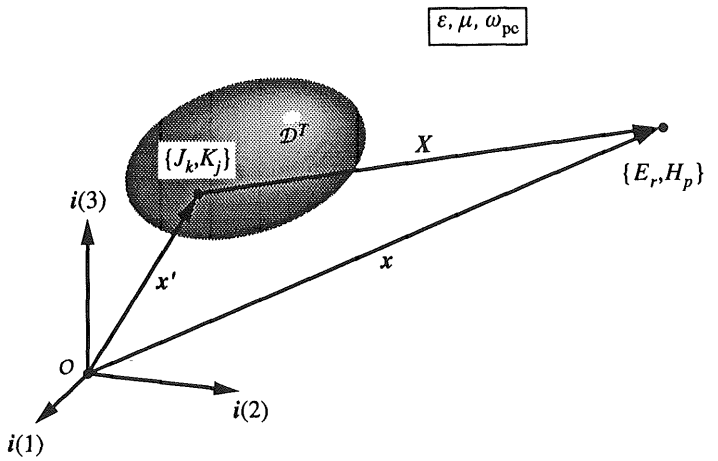

Figure 26.8-1 Time-domain source-type integral representations for the electromagnetic field $\{E_r, H_p\}$ observed at position $x \in \mathcal{R}^3$, radiated by source distributions $\{J_k, K_j\}$ at position $x \in \mathcal{D}^T$ (bounded source domain) in an unbounded, homogeneous, isotropic electron plasma or a superconducting metal, with electron plasma angular frequency ω_{pe}.

With this the time-domain expressions for the electric and magnetic field strengths radiated by sources in a homogeneous, isotropic collisionless plasma in a vacuum background (or a superconducting metal) have been completed.

26.9 The electromagnetic field emitted by a short segment of a thin, conducting, current-carrying wire

In this section we calculate the electric and the magnetic field strengths of the electromagnetic field emitted by a short segment of a thin, conducting, current-carrying wire. First of all, conducting wires are only capable of carrying electric volume currents and carry no magnetic volume currents. Consequently, $K_j = 0$ and, hence, $\Phi_j^K = 0$. Furthermore, in the thin-wire approximation, we replace the actual volume distribution of electric current by a wire current concentrated at the centre wire of the conductor, the wire current having the direction of the local tangent to the wire segment (Figure 26.9-1).

Complex frequency-domain electromagnetic field expressions

Let $\hat{I} = \hat{I}(x,s)$ denote the complex frequency-domain magnitude of the electric wire current and let dx_k be the vectorial wire element of the centre wire $\mathcal{L}$ of the conducting wire, then for points not too close to the wire we have (see Equation (26.3-3))

$$\hat{\Phi}_k^J(x,s) = \int_{x' \in \mathcal{L}} \hat{G}(x-x',s)\hat{I}(x',s)\, dx'_k \,. \tag{26.9-1}$$

The expressions of Equations (26.3-1) and (26.3-2) for the electric and the magnetic field strengths reduce in the present case to

$$\hat{E}_k = -\hat{\zeta}\hat{\Phi}_k^J + \hat{\eta}^{-1}\partial_k\partial_r\hat{\Phi}_r^J \,, \tag{26.9-2}$$

and

$$\hat{H}_j = \varepsilon_{j,n,r}\partial_n\hat{\Phi}_r^J \,. \tag{26.9-3}$$

For a short segment of a conducting wire centred around the point $x' = b$ (for example, its barycentre), carrying a uniform current $\hat{I} = \hat{I}(s)$, and for points not too close to the conductor, the expression for $\hat{\Phi}_k^J$ can be approximated by

$$\hat{\Phi}_k^J = \hat{I}L_k \exp(-\hat{\gamma}|X|)/4\pi|X| \,, \tag{26.9-4}$$

where L_k is the vectorial length of the wire segment and

$$X = x - b \tag{26.9-5}$$

is the position vector from the reference point around which the wire segment is centred to the point of observation (Figure 26.9-2). Substitution of Equation (26.9-4) in Equations (26.9-2) and (26.9-3) leads to expressions for $\hat{E}_k$ and $\hat{H}_j$ that can be written as (see Equations (26.3-9)–(26.3-16))

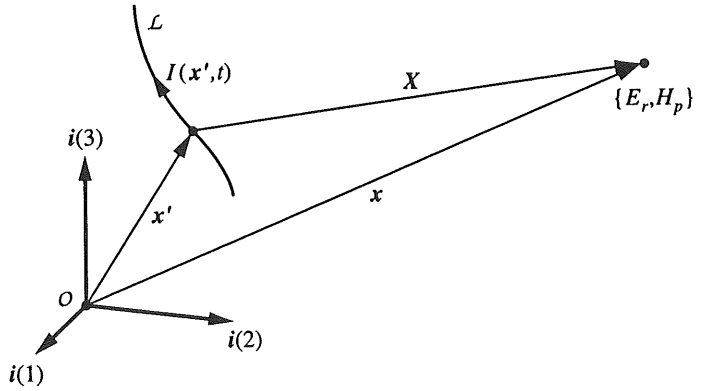

Figure 26.9-1 Electromagnetic radiation from a segment of a conducting, current-carrying wire $\mathcal{L}$. $I = I(x,t)$ is the electric current in the wire.

$$\hat{E}_k = \hat{E}_k^{\mathrm{NF}} + \hat{E}_k^{\mathrm{IF}} + \hat{E}_k^{\mathrm{FF}}, \tag{26.9-6}$$

and

$$\hat{H}_j = \hat{H}_j^{\mathrm{IF}} + \hat{H}_j^{\mathrm{FF}}, \tag{26.9-7}$$

where the electric near-field contribution is given by

$$\hat{E}_k^{\mathrm{NF}}(x,s) = \hat{\eta}^{-1}(3\Xi_k\Xi_r - \delta_{k,r})\hat{I}(s)L_r \frac{\exp(-\hat{\gamma}|X|)}{4\pi|X|^3}, \tag{26.9-8}$$

the electric intermediate-field contribution by

$$\hat{E}_k^{\mathrm{IF}}(x,s) = (\hat{\gamma}/\hat{\eta})(3\Xi_k\Xi_r - \delta_{k,r})\hat{I}(s)L_r \frac{\exp(-\hat{\gamma}|X|)}{4\pi|X|^2}, \tag{26.9-9}$$

the electric far-field contribution by

$$\hat{E}_k^{\mathrm{FF}}(x,s) = \hat{\zeta}(\Xi_k\Xi_r - \delta_{k,r})\hat{I}(s)L_r \frac{\exp(-\hat{\gamma}|X|)}{4\pi|X|}, \tag{26.9-10}$$

the magnetic intermediate-field contribution by

$$\hat{H}_j^{\mathrm{IF}}(x,s) = -\varepsilon_{j,n,r}\Xi_n\hat{I}(s)L_r \frac{\exp(-\hat{\gamma}|X|)}{4\pi|X|^2}, \tag{26.9-11}$$

and the magnetic far-field contribution by

$$\hat{H}_j^{\mathrm{FF}}(x,s) = -\hat{\gamma}\varepsilon_{j,n,r}\Xi_n\hat{I}(s)L_r \frac{\exp(-\hat{\gamma}|X|)}{4\pi|X|}. \tag{26.9-12}$$

In these expressions, X is given by Equation (26.9-5) and

$$\Xi_m = X_m/|X| \tag{26.9-13}$$

is the unit vector in the direction of X. Note that there is no near-field contribution to the magnetic field.

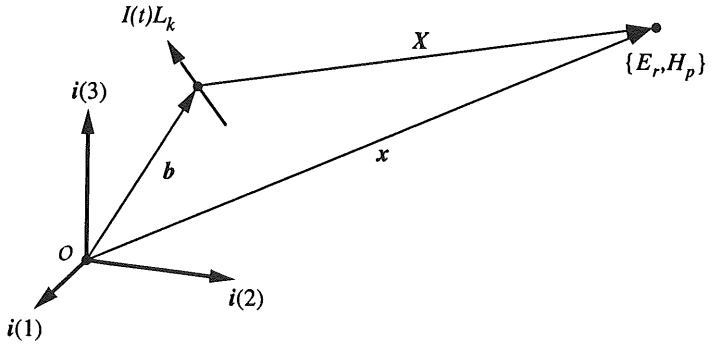

Figure 26.9-2 Electromagnetic radiation from a short segment of a conducting, current-carrying wire $\mathcal{L}$. $I = I(t)$ is the (uniform) electric current in the wire; $\boldsymbol{L}$ is the vectorial length of the wire segment and $\boldsymbol{b}$ is the point about which the wire segment is centred.

All expressions have the complex frequency-domain propagation factor $\exp(-\hat{\gamma}|\boldsymbol{X}|)$ in common. As far as the distance of the point of observation from the source is concerned, the near field is proportional to (distance)$^{-3}$, the intermediate field proportional to (distance))$^{-2}$, and the far field proportional to (distance)$^{-1}$. Furthermore, each field constituent exhibits a particular directional pattern in which the polar near-field and intermediate field directional patterns $3\Xi_k\Xi_r - \delta_{k,r}$, the polar far-field pattern $\Xi_k\Xi_r - \delta_{k,r}$ and the axial intermediate field and far-field patterns $-\varepsilon_{j,n,r}\Xi_n$ occur. The electric field is oriented in the plane through the current-carrying conducting wire segment and the point of observation. The magnetic field is oriented normal to the plane through the point of observation and the current-carrying conducting wire segment.

Let θ denote the angle included between $\boldsymbol{L}$ and $\boldsymbol{X}$, then we have for the magnitudes of the directional patterns (Figures 26.9-3–26.9-5)

$$\begin{aligned}|3\Xi_k\Xi_rL_r - L_k| &= [(3\Xi_k\Xi_rL_r - L_k)(3\Xi_k\Xi_{r'}L_{r'} - L_k)]^{1/2}\\ &= [9(\Xi_rL_r)^2 - 3(\Xi_kL_k)^2 - 3(\Xi_rL_r)^2 + L_kL_k]^{1/2}\\ &= [3(\Xi_rL_r)^2 + L_kL_k]^{1/2}\\ &= [3|\boldsymbol{L}|^2\cos^2(\theta) + |\boldsymbol{L}|^2]^{1/2}\\ &= |\boldsymbol{L}|[3\cos^2(\theta) + 1]^{1/2},\end{aligned} \tag{26.9-14}$$

and

$$\begin{aligned}|\Xi_k\Xi_rL_r - L_k| &= [(\Xi_k\Xi_rL_r - L_k)(\Xi_k\Xi_{r'}L_{r'} - L_k)]^{1/2}\\ &= [(\Xi_rL_r)^2 - (\Xi_kL_k)^2 - (\Xi_rL_r)^2 + L_kL_k]^{1/2}\\ &= [L_kL_k - (\Xi_rL_r)^2]^{1/2}\\ &= [|\boldsymbol{L}|^2 - |\boldsymbol{L}|^2\cos^2(\theta)]^{1/2}\\ &= |\boldsymbol{L}||\sin(\theta)|,\end{aligned} \tag{26.9-15}$$

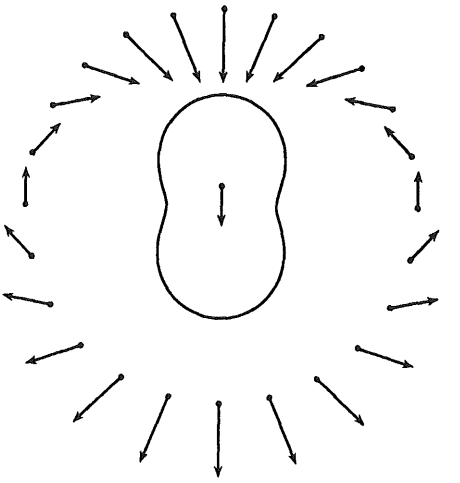

Figure 26.9-3 Near-field and intermediate-field polar radiation characteristic $3L_r\Xi_r\Xi_k - L_k$.

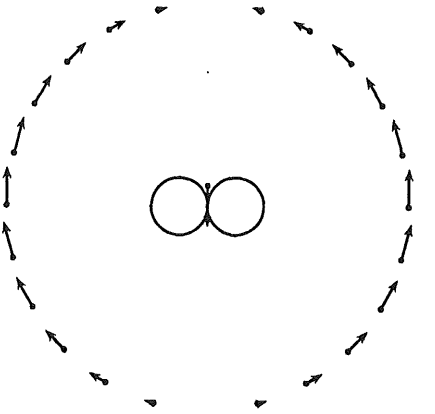

Figure 26.9-4 Far-field polar radiation characteristic $\Xi_k\Xi_r L_r - L_k$.

and

$$
\begin{aligned}
|\varepsilon_{j,n,r}\Xi_n L_r| &= (\varepsilon_{j,n,r}\Xi_n L_r \varepsilon_{j,n',r'}\Xi_{n'}L_{r'})^{1/2} \\
&= [(\delta_{n,n'}\delta_{r,r'} - \delta_{n,r'}\delta_{r,n'})\Xi_n L_r \Xi_{n'}L_{r'}]^{1/2} \\
&= [L_r L_r - \Xi_{r'}L_r\Xi_r L_{r'}]^{1/2} \\
&= [L_r L_r - (\Xi_r L_r)^2]^{1/2} \\
&= [|L|^2 - |L|^2\cos^2(\theta)]^{1/2} \\
&= |L||\sin(\theta)|\,. \qquad (26.9\text{-}16)
\end{aligned}
$$

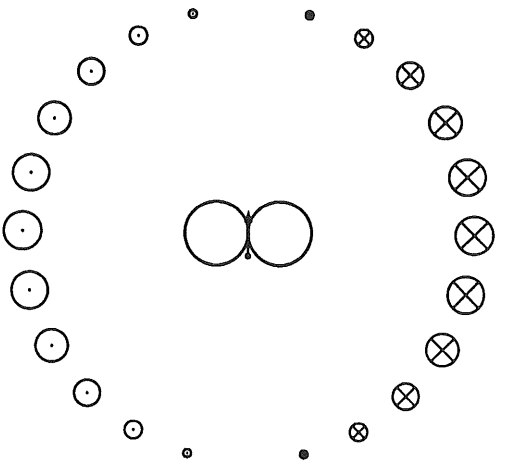

Figure 26.9-5 Intermediate-field and far-field axial radiation characteristic $-\varepsilon_{j,n,r}\Xi_n L_r$.

All directional patterns are rotationally symmetrical around the axis of the current-carrying conducting wire segment.

Time-domain electromagnetic field expressions for a lossless medium

For the field emission in a homogeneous, isotropic and lossless medium with permittivity ε, permeability μ and electromagnetic wave speed $c = (\varepsilon\mu)^{-1/2}$, the corresponding time-domain expressions easily follow from the complex frequency-domain results by applying some standard rules of the time Laplace transformation. The result is written as (see Equations (26.9-6)–(26.9-12))

$$E_k = E_k^{\mathrm{NF}} + E_k^{\mathrm{IF}} + E_k^{\mathrm{FF}}, \tag{26.9-17}$$

and

$$H_j = H_j^{\mathrm{IF}} + H_j^{\mathrm{FF}}, \tag{26.9-18}$$

in which the electric near-field contribution is given by

$$E_k^{\mathrm{NF}}(x,t) = \varepsilon^{-1}(3\Xi_k\Xi_r - \delta_{k,r})L_r \frac{\mathrm{I}_t I(t-|X|/c)}{4\pi|X|^3}, \tag{26.9-19}$$

the electric intermediate-field contribution by

$$E_k^{\mathrm{IF}}(x,t) = (\varepsilon c)^{-1}(3\Xi_k\Xi_r - \delta_{k,r})L_r \frac{I(t-|X|/c)}{4\pi|X|^2}, \tag{26.9-20}$$

the electric far-field contribution by

$$E_k^{\mathrm{FF}}(x,t) = \mu(\Xi_k \Xi_r - \delta_{k,r}) L_r \frac{\partial_t I(t - |X|/c)}{4\pi |X|}, \tag{26.9-21}$$

the magnetic intermediate-field contribution by

$$H_j^{\mathrm{IF}}(x,t) = -\varepsilon_{j,n,r} \Xi_n L_r \frac{I(t - |X|/c)}{4\pi |X|^2}, \tag{26.9-22}$$

and the magnetic far-field contribution by

$$H_j^{\mathrm{FF}}(x,t) = -c^{-1} \varepsilon_{j,n,r} \Xi_n L_r \frac{\partial_t I(t - |X|/c)}{4\pi |X|}, \tag{26.9-23}$$

while there is no magnetic near-field contribution.

All time-domain expressions contain the travel-time delay $|X|/c$. With regard to the dependence of the different terms on the distance of the source point $\boldsymbol{b}$ to an observation point $\boldsymbol{x}$ and the directional patterns of the different terms, the same remarks as for the complex frequency-domain results apply. The short segment of a conducting wire carrying a uniform electric current is also denoted as a radiating *electric dipole*, with moment $\hat{I}(s)L_r$ or $I(t)L_r$.

In many electronic devices, equipment or systems that operate in the quasi-static regime and are designed at the basis of the Kirchhoff voltage and electric current laws of electric circuit theory, the emission of electromagnetic radiation by the current-carrying conductors or circuit elements is an unwanted effect that may degrade the performance of the devices, equipment or systems in their electromagnetic environment. This aspect of ElectroMagnetic Compatibility (EMC) will be further discussed in Chapter 30.

For the results of this section to be applicable, the wire segment should be short compared to the smallest wavelength in the frequency spectrum of the applied electric current (frequency-domain description) or short compared to the minimum spatial extent of the field emitted by the applied electric current pulse (time-domain description).

26.10 The electromagnetic field emitted by small, conducting, current-carrying loop

In this section we calculate the electric and the magnetic field strengths of the electromagnetic field emitted by a small, conducting, current-carrying wire in the shape of a loop (Figure 26.10-1). Again $K_j = 0$ and, hence, $\Phi_j^K = 0$. Here, too, the thin-wire approximation is used, in which the actual volume distribution of electric current is replaced by a wire current concentrated at the centre wire of the loop, the wire current having the direction of the local tangent to the loop.

Complex frequency-domain electromagnetic field expressions

For a conducting loop C carrying a uniform electric current of magnitude $\hat{I} = \hat{I}(s)$ and for points of observation not too close to the loop, the expression Equation (26.9-1) for the electric current volume-source vector potential reduces to

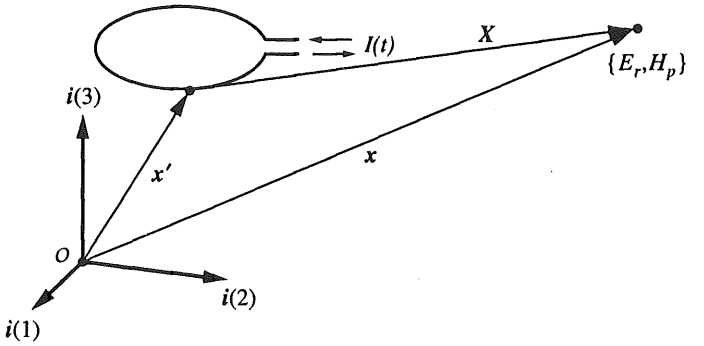

Figure 26.10-1 Electromagnetic radiation from a small, conducting, current-carrying loop C. $I = I(t)$ is the (uniform) electric current in the loop; A is the vectorial area of the loop.

$$\hat{\Phi}_k^J(\boldsymbol{x},s) = \hat{I}(s) \oint_{x' \in C} \hat{G}(\boldsymbol{x} - \boldsymbol{x}', s)\, \mathrm{d}x_k' \,. \tag{26.10-1}$$

Let now $\boldsymbol{b}$ be the position vector of some fixed point close to the loop (for example, its barycentre). Then, for a small loop, the integral on the right-hand side of Equation (26.10-1) can be approximated by using the zeroth- and first-order terms of the Taylor expansion of $\hat{G}$ in $\boldsymbol{x}'$ about $\boldsymbol{b}$ (Figure 26.10-2). Using the property

$$\hat{G}(\boldsymbol{x} - \boldsymbol{x}', s) = \hat{G}(\boldsymbol{x} - \boldsymbol{b} + \boldsymbol{b} - \boldsymbol{x}', s) = \hat{G}[\boldsymbol{x} - \boldsymbol{b} - (\boldsymbol{x}' - \boldsymbol{b}), s] \,, \tag{26.10-2}$$

we have the Taylor expansion

$$\hat{G}[\boldsymbol{x} - \boldsymbol{b} - (\boldsymbol{x}' - \boldsymbol{b}), s] = \hat{G}(\boldsymbol{x} - \boldsymbol{b}, s) - (x_m' - b)\partial_m \hat{G}(\boldsymbol{x} - \boldsymbol{b}, s) + o(|\boldsymbol{x}' - \boldsymbol{b}|)$$

$$\text{as} \quad |\boldsymbol{x}' - \boldsymbol{b}| \to 0 \,, \tag{26.10-3}$$

about $\boldsymbol{x}' = \boldsymbol{b}$. Since

$$\oint_{x' \in C} \mathrm{d}x_k' = 0 \,, \tag{26.10-4}$$

because of the fact that C is a closed loop, substitution of Equation (26.10-3) in Equation (26.10-1) leads to

$$\hat{\Phi}_k^J(\boldsymbol{x},s) = -\hat{I}(s)\partial_m \hat{G}(\boldsymbol{x} - \boldsymbol{b}, s) \oint_{x' \in C} (x_m' - b_m)\mathrm{d}x_k' \,, \tag{26.10-5}$$

or, using Stokes' theorem of vector analysis (see Exercise 26.10-1),

$$\hat{\Phi}_k^J(\boldsymbol{x},s) = -\varepsilon_{k,p,m}\hat{I}(s)\partial_m \hat{G}(\boldsymbol{x} - \boldsymbol{b}, s) \int_{x' \in S} \mathrm{d}A_p \,, \tag{26.10-6}$$

where the integral on the right-hand side is the vectorial area of the loop C and is extended over some two-sided surface S of which C is the boundary curve. Introducing

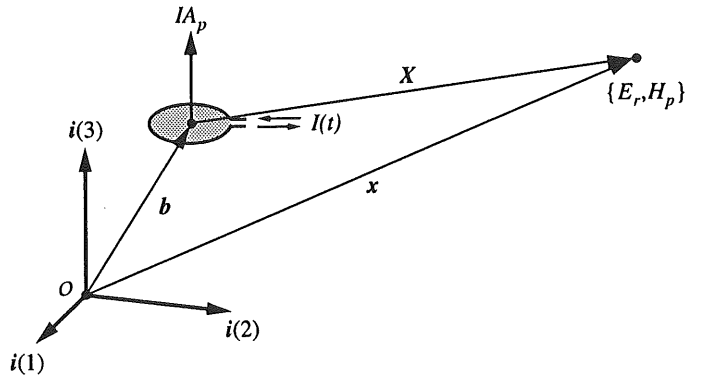

Figure 26.10-2 Electromagnetic radiation from a small, conducting, current-carrying loop C. $I = I(t)$ is the (uniform) electric current in the loop; $\boldsymbol{A}$ is the vectorial area of the loop and $\boldsymbol{b}$ is the point about which the loop is centred.

$$\hat{m}_p(s) = \hat{I}(s) \int_{x' \in S} dA_p \tag{26.10-7}$$

as the *magnetic moment of the loop*, we can rewrite Equation (26.10-6) as

$$\hat{\Phi}_k^J(\boldsymbol{x},s) = \varepsilon_{k,m,p}\partial_m\left[\hat{m}_p(s)\hat{G}(\boldsymbol{x}-\boldsymbol{b},s)\right]. \tag{26.10-8}$$

Now, since $\partial_k(\varepsilon_{k,m,p}\partial_m) = 0$ it is easily verified that

$$\partial_k\hat{\Phi}_k^J = 0\,. \tag{26.10-9}$$

Furthermore,

$$\begin{aligned}\varepsilon_{j,n,r}\partial_n\hat{\Phi}_r^J &= \varepsilon_{j,n,r}\varepsilon_{r,m,p}\partial_n\partial_m\left[\hat{m}_p(s)\hat{G}(\boldsymbol{x}-\boldsymbol{b},s)\right]\\ &= (\delta_{j,m}\delta_{n,p} - \delta_{j,p}\delta_{n,m})\partial_n\partial_m\left[\hat{m}_p(s)\hat{G}(\boldsymbol{x}-\boldsymbol{b},s)\right]\\ &= \partial_j\partial_p\left[\hat{m}_p(s)\hat{G}(\boldsymbol{x}-\boldsymbol{b},s)\right] - \partial_m\partial_m\left[\hat{m}_j(s)\hat{G}(\boldsymbol{x}-\boldsymbol{b},s)\right]\\ &= \partial_j\partial_p\left[\hat{m}_p(s)\hat{G}(\boldsymbol{x}-\boldsymbol{b},s)\right] - \hat{\gamma}^2\hat{m}_j(s)\hat{G}(\boldsymbol{x}-\boldsymbol{b},s) \quad \text{for } \boldsymbol{x}-\boldsymbol{b} \neq 0\,,\end{aligned} \tag{26.10-10}$$

where Equation (26.2-4) has been used. Substitution of Equations (26.10-8)–(26.10-10) in Equations (26.9-2) and (26.9-3) yields

$$\hat{E}_k = -\hat{\zeta}\varepsilon_{k,m,p}\partial_m\left[\hat{m}_p(s)\hat{G}(\boldsymbol{x}-\boldsymbol{b},s)\right], \tag{26.10-11}$$

and

$$\hat{H}_j = -\hat{\gamma}^2\hat{m}_j(s)\hat{G}(\boldsymbol{x}-\boldsymbol{b},s) + \partial_j\partial_p\left[\hat{m}_p(s)\hat{G}(\boldsymbol{x}-\boldsymbol{b},s)\right]. \tag{26.10-12}$$

Comparison of Equations (26.10-11) and (26.10-12) with Equations (26.3-1) and (26.3-2) shows that the resulting electromagnetic field can be considered as due to a magnetic current volume source vector potential having the value

$$\hat{\Phi}_p^K = \hat{\zeta}\hat{m}_p(s)\hat{G}(\boldsymbol{x}-\boldsymbol{b},s)\,. \tag{26.10-13}$$

For this reason, the small, current-carrying conducting loop is also denoted as a *magnetic dipole*. Substitution of Equation (26.10-13) in Equations (26.10-11) and (26.10-12) leads to

$$\hat{E}_k = -\varepsilon_{k,m,p}\partial_m \hat{\Phi}_p^K, \tag{26.10-14}$$

and

$$\hat{H}_j = -\hat{\eta}\hat{\Phi}_j^K + \hat{\zeta}^{-1}\partial_j\partial_p\hat{\Phi}_p^K. \tag{26.10-15}$$

The further use of Equations (26.3-11)–(26.3-16) leads to

$$\hat{E}_k = \hat{E}_k^{\mathrm{IF}} + \hat{E}_k^{\mathrm{FF}}, \tag{26.10-16}$$

and

$$\hat{H}_j = \hat{H}_j^{\mathrm{NF}} + \hat{H}_j^{IF} + \hat{H}_j^{\mathrm{FF}}, \tag{26.10-17}$$

where the electric intermediate-field contribution is given by

$$\hat{E}_k^{\mathrm{IF}}(x,s) = \hat{\zeta}\varepsilon_{k,m,p}\Xi_m\hat{m}_p(s)\frac{\exp(-\hat{\gamma}|X|)}{4\pi|X|^2}, \tag{26.10-18}$$

the electric far-field contribution by

$$\hat{E}_k^{\mathrm{FF}}(x,s) = \hat{\gamma}\hat{\zeta}\varepsilon_{k,m,p}\Xi_m\hat{m}_p(s)\frac{\exp(-\hat{\gamma}|X|)}{4\pi|X|}, \tag{26.10-19}$$

the magnetic near-field contribution by

$$\hat{H}_j^{\mathrm{NF}}(x,s) = (3\Xi_j\Xi_p - \delta_{j,p})\hat{m}_p(s)\frac{\exp(-\hat{\gamma}|X|)}{4\pi|X|^3}, \tag{26.10-20}$$

the magnetic intermediate-field contribution by

$$\hat{H}_j^{\mathrm{IF}}(x,s) = \hat{\gamma}(3\Xi_j\Xi_p - \delta_{j,p})\hat{m}_p(s)\frac{\exp(-\hat{\gamma}|X|)}{4\pi|X|^2}, \tag{26.10-21}$$

and the magnetic far-field contribution by

$$\hat{H}_j^{\mathrm{FF}}(x,s) = \hat{\gamma}^2(\Xi_j\Xi_p - \delta_{j,p})\hat{m}_p(s)\frac{\exp(-\hat{\gamma}|X|)}{4\pi|X|}, \tag{26.10-22}$$

while there is no electric near-field contribution.

In these expressions,

$$X = x - b \tag{26.10-23}$$

is the vectorial distance from the chosen centre of the loop to the point of observation, and

$$\Xi_j = X_j/|X| \tag{26.10-24}$$

is the unit vector oriented from the chosen centre of the loop to the point of observation.

As far the complex frequency-domain propagation factor, the dependence on the distance between source and observation point and the directional patterns are concerned, the same remarks as for the electromagnetic field emitted by a short, conducting, current-carrying wire segment apply, be it that the roles of electric field and magnetic field are interchanged.

Time-domain electromagnetic field expressions for a lossless medium

For the field emission in a homogeneous, isotropic and lossless medium with permittivity ε, permeability μ and electromagnetic wave speed $c = (\varepsilon\mu)^{-1/2}$ the corresponding time-domain expressions easily follow from the complex frequency-domain results by applying some standard rules of the time Laplace transformation. The result is written as (see Equations (26.10-16)–(26.10-22))

$$E_k = E_k^{\mathrm{IF}} + E_k^{\mathrm{FF}} \tag{26.10-25}$$

and

$$H_j = H_j^{\mathrm{NF}} + H_j^{\mathrm{IF}} + H_j^{\mathrm{FF}}, \tag{26.10-26}$$

where the electric intermediate-field contribution is given by

$$E_k^{\mathrm{IF}}(x,t) = \mu\varepsilon_{k,m,p}\Xi_m A_p \frac{\partial_t I(t-|X|/c)}{4\pi|X|^2}, \tag{26.10-27}$$

the electric far-field contribution by

$$E_k^{\mathrm{FF}}(x,t) = \mu c^{-1}\varepsilon_{k,m,p}\Xi_m A_p \frac{\partial_t^2 I(t-|X|/c)}{4\pi|X|}, \tag{26.10-28}$$

the magnetic near-field contribution by

$$H_j^{\mathrm{NF}}(x,t) = (3\Xi_j\Xi_p - \delta_{j,p})A_p \frac{I(t-|X|/c)}{4\pi|X|^3}, \tag{26.10-29}$$

the magnetic intermediate-field contribution by

$$H_j^{\mathrm{IF}}(x,t) = c^{-1}(3\Xi_j\Xi_p - \delta_{j,p})A_p \frac{\partial_t I(t-|X|/c)}{4\pi|X|^2}, \tag{26.10-30}$$

and the magnetic far-field contribution by

$$H_j^{\mathrm{FF}}(x,st = c^{-2}(\Xi_j\Xi_p - \delta_{j,p})A_p \frac{\partial_t^2 I(t-|X|/c)}{4\pi|X|}, \tag{26.10-31}$$

while there is no electric near-field contribution.

In these expressions

$$A_p = \int_{x' \in S} \mathrm{d}A_p \tag{26.10-32}$$

is the vectorial area of the loop C.

As to the travel-time delay and other characteristics of the different terms, the same remarks as in Section 26.9 apply.

In many electronic devices, equipment or systems that operate in the quasi-static regime and are designed at the basis of the Kirchhoff voltage and electric current laws of electric circuit theory, the emission of electromagnetic radiation by the current-carrying conductors or circuit elements is an unwanted effect that may degrade the performance of the devices, equipment or

systems in their electromagnetic environment. This aspect of ElectroMagnetic Compatibility (EMC) will be further discussed in Chapter 30.

For the results of this section to be applicible, the dimensions of the loop should be small compared to the smallest wavelength in the frequency spectrum of the applied electric current (frequency-domain description) or small compared to the minimum spatial extent of the field emitted by the applied electric current pulse (time-domain description).

Exercises

Exercise 26.10-1

Let C be a bounded closed curve in $\mathcal{R}^3$ and let S be some bounded two-sided surface that has C as boundary curve. Let, further, $\phi = \phi(x)$ be a function that is continuously differentiable in the neighbourhood of S. Then

$$\int_{x \in C} \phi \, dx_p = \varepsilon_{p,r,q} \int_{x \in S} \partial_q \phi \, dA_r \tag{26.10-33}$$

(Stokes' theorem), where the direction of circulation along C and the orientation of dA_r form a right-handed system. Use Equation (26.10-33) to prove the step leading from Equation (26.10-5) to Equation (26.10-6). Equation (26.10-33) can be proved by subdividing S into a number of (small) planar triangles and applying the two-dimensional form of Gauss' theorem (see Section A.9) to the interior of each triangle.

26.11 Far-field radiation characteristics of extended sources (complex frequency-domain analysis)

In many applications of electromagnetic radiation (for example, in telecommunications and in radio and television broadcasting) one is often particularly interested in the behaviour of the radiated field at large distances from the radiating structures. To investigate this behaviour, we consider the leading term in the expansion of the right-hand sides of Equation (26.3-1)–(26.3-5) as $|x| \to \infty$; this term is denoted as the *far-field approximation* of the relevant electromagnetic field. The region in space where the far-field approximation represents the wave-field values with sufficient accuracy is denoted as the *far-field region*. Since in the far-field region the mutual relationship between the electric and the magnetic field strengths (though not their radiation characteristics) prove to be the same for the field constituents generated by electric-current sources and the field constituents generated by magnetic-current sources, it is advantageous to investigate these relationships for the total field, which will be done below.

To construct the far-field approximation we first observe that

$$|x - x'| = [(x_s - x'_s)(x_s - x'_s)]^{1/2} = |x| \, [1 - 2x_s x'_s / |x|^2 + |x'|^2 / |x|^2]^{1/2}, \tag{26.11-1}$$

from which by a Taylor expansion of the square-root expression about $|x| = \infty$, it follows that (Figure 26.11-1)

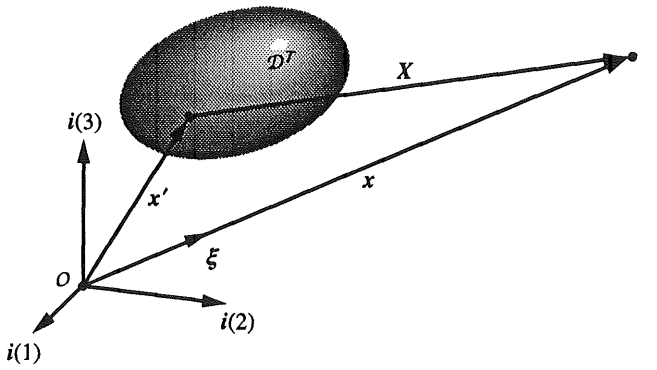

Figure 26.11-1 Far-field approximation to the distance function from source point $x' \in \mathcal{D}^T$ to observation point $x \in \mathcal{R}^3$: $|X| = |x - x'| = |x| - \xi_s x_s' + O(|x|^{-1})$ as $|x| \to \infty$.

$$|x - x'| = |x| - \xi_s x_s' + O(|x|^{-1}) \qquad \text{as } |x| \to \infty , \tag{26.11-2}$$

where

$$\xi_s = x_s/|x| \tag{26.11-3}$$

is the unit vector in the direction of observation (note that in the far-field region certainly $|x| \neq 0$). For the derivatives of $|x - x'|$ furthermore, we have

$$\partial_m |x - x'| = (x_m - x_m')/|x - x'| . \tag{26.11-4}$$

This leads to

$$\partial_m |x - x'| = \xi_m + O(|x|^{-1}) \qquad \text{as } |x| \to \infty , \tag{26.11-5}$$

where the Order term follows from a Taylor expansion of $|(x_m - x_m')/|x - x'| - \xi_m|$ about $|x| = \infty$. Using these results, the Green's function of the scalar Helmholtz equation, Equation (26.3-5), can, in the far-field region, be approximated by

$$\hat{G}(x - x', s) = \frac{\exp(-\hat{\gamma}|x|)}{4\pi|x|} \exp(\hat{\gamma}\xi_s x_s') \, [1 + O(|x|^{-1})] \qquad \text{as } |x| \to \infty , \tag{26.11-6}$$

and its spatial derivatives by

$$\partial_m \hat{G}(x - x', s) = (-\hat{\gamma}\xi_m) \frac{\exp(-\hat{\gamma}|x|)}{4\pi|x|} \exp(\hat{\gamma}\xi_s x_s') \, [1 + O(|x|^{-1})] \qquad \text{as } |x| \to \infty . \tag{26.11-7}$$

Using Equation (26.11-6) in the expressions for the electric-current and magnetic-current source vector potentials, Equations (26.3-3) and (26.3-4), we obtain their far-field approximations as

$$\{\hat{\Phi}_r^J, \hat{\Phi}_p^K\}(x,s) = \{\hat{\Phi}_r^{J;\infty}, \hat{\Phi}_p^{K;\infty}\}(\xi,s) \frac{\exp(-\hat{\gamma}|x|)}{4\pi|x|} [1 + O(|x|^{-1})] \qquad \text{as } |x| \to \infty , \tag{26.11-8}$$

in which

$$\{\hat{\Phi}_r^{J;\infty},\hat{\Phi}_p^{K;\infty}\}(\xi,s) = \int_{x'\in\mathcal{D}^T} \exp(\hat{\gamma}\xi_s x'_s)\{\hat{J}_r,\hat{K}_p\}(x',s)\,\mathrm{d}V\,. \tag{26.11-9}$$

Using Equations (26.11-7)–(26.11-9) in the expressions of Equations (26.3-1) and (26.3-2) for the electric and the magnetic field strengths, we obtain the latter's far-field approximations as

$$\{\hat{E}_k,\hat{H}_j\}(x,s) = \{\hat{E}_k^{\infty},\hat{H}_j^{\infty}\}(\xi,s)\,\frac{\exp(-\hat{\gamma}|x|)}{4\pi|x|}\,[1+O(|x|^{-1})] \quad \text{as } |x|\to\infty\,, \tag{26.11-10}$$

in which

$$\hat{E}_k^{\infty} = \hat{\zeta}(\xi_k\xi_r - \delta_{k,r})\hat{\Phi}_r^{J;\infty} + \varepsilon_{k,m,p}\hat{\gamma}\xi_m\hat{\Phi}_p^{K;\infty}, \tag{26.11-11}$$

and

$$\hat{H}_j^{\infty} = \hat{\eta}(\xi_j\xi_p - \delta_{j,p})\hat{\Phi}_p^{K;\infty} - \varepsilon_{j,n,r}\hat{\gamma}\xi_n\hat{\Phi}_r^{J;\infty}. \tag{26.11-12}$$

As Equation (26.11-10) shows, the electric and the magnetic field strengths have, in the far-field region, the structure of a spherical wave that expands radially from the origin of the coordinate system (which is also denoted as the *phase centre* of the far-field approximation), the latter being chosen in the neighbourhood of the radiating sources, with an amplitude that depends on the direction of observation and that decreases inversely proportionally to the distance from the sources. The amplitude radiation characteristics $\{\hat{E}_k^{\infty},\hat{H}_j^{\infty}\}$ depend only on the direction of observation ξ and on s. Their dependence on ξ is the resultant of the dependence of the integrals occurring in the right-hand side of Equation (26.11-9) on ξ, and the electromagnetic far-field polar and axial radiation characteristics $\xi_k\xi_r - \delta_{k,r}$ and $-\varepsilon_{j,n,r}\xi_n$.

The far-field amplitude radiation characteristics of the electric and the magnetic field strengths are not independent of each other. It is easily verified that the right-hand sides of Equations (26.11-11) and (26.11-12) are interrelated in the following way:

$$\varepsilon_{k,m,p}\hat{\gamma}\xi_m\hat{H}_p^{\infty} + \hat{\eta}\hat{E}_k^{\infty} = 0\,, \tag{26.11-13}$$

$$-\varepsilon_{j,n,r}\hat{\gamma}\xi_n\hat{E}_r^{\infty} + \hat{\zeta}\hat{H}_j^{\infty} = 0\,. \tag{26.11-14}$$

Now, relations of the kind of Equations (26.11-13) and (26.11-14) would also have resulted if expressions of the type

$$\{\hat{E}_k,\hat{H}_j\} = \{\hat{E}_k^{\infty},\hat{H}_j^{\infty}\}\exp(-\hat{\gamma}\xi_s x_s)\,, \tag{26.11-15}$$

where $\hat{E}_k^{\infty}$ and $\hat{H}_j^{\infty}$ only depend on the real unit vector ξ and the time Laplace-transform parameter s and not on x, had been substituted in the source-free electromagnetic field equations pertaining to the homogeneous, isotropic medium under consideration. Wave fields of the type of Equation (26.11-15) are denoted as complex frequency-domain *uniform plane waves*. Observing that $|x| = \xi_s x_s$, we can therefore say that, after compensating for the (distance)$^{-1}$ decay, the spherical-wave amplitudes in the far-field radiation pattern behave locally (i.e. for a fixed direction of observation ξ) as if the wave were a uniform plane wave travelling in the radial direction away from the source.

To exhibit the further properties of $\{\hat{E}_k^{\infty},\hat{H}_j^{\infty}\}$ we rewrite Equations (26.11-13) and (26.11-14) as

$$\varepsilon_{k,m,p}\xi_m\hat{H}_p^{\infty} + \hat{Y}\hat{E}_k^{\infty} = 0\,, \tag{26.11-16}$$

$$-\varepsilon_{j,n,r}\xi_n\hat{E}_r^{\infty} + \hat{Z}\hat{H}_j^{\infty} = 0\,, \tag{26.11-17}$$

in which

$$\hat{Y} = (\hat{\eta}/\hat{\zeta})^{1/2} \tag{26.11-18}$$

is the *electromagnetic plane wave admittance* and

$$\hat{Z} = (\hat{\zeta}/\hat{\eta})^{1/2} \tag{26.11-19}$$

is the *electromagnetic plane wave impedance* of the medium under consideration. Contraction of Equation (26.11-16) with ξ_k and of Equation (26.11-17) with ξ_j leads to

$$\xi_k\hat{E}_k^{\infty} = 0 \tag{26.11-20}$$

and

$$\xi_j\hat{H}_j^{\infty} = 0\,, \tag{26.11-21}$$

respectively. Hence, the electric and the magnetic field strengths in the far-field region are *transverse with respect to the radial direction of propagation* of the wave, and are, since $\varepsilon_{k,m,p}$ and ξ_m have unit magnitudes, proportional with proportionality factors $\hat{Y}$ or $\hat{Z}$.

Upon inspecting the dependence of the integrals occurring in the expressions for $\hat{\Phi}_k^{J;\infty}$ and $\hat{\Phi}_j^{K;\infty}$ on $\boldsymbol{\xi}$, a comparison of Equation (26.11-9) with Equation (26.1-11) shows that

$$\{\hat{\Phi}_k^{J;\infty}, \hat{\Phi}_j^{K;\infty}\}(\boldsymbol{\xi}, s) = \{\tilde{J}_k, \tilde{K}_j\}(\hat{\gamma}\boldsymbol{\xi}, s)\,. \tag{26.11-22}$$

Consequently, in the far-field region only the spatial Fourier transforms of the source distributions at the subset of angular wave-vector values $j\boldsymbol{k} = \hat{\gamma}\boldsymbol{\xi}$ are "visible".

Exercises

Exercise 26.11-1

Verify that Equations (26.11-11) and (26.11-12) indeed satisfy Equations (26.11-13) and (26.11-14).

26.12 Far-field radiation characteristics of extended sources (time-domain analysis for a lossless medium)

In this section we investigate the time-domain far-field radiation characteristics of the electromagnetic field generated by extended sources immersed in a homogeneous, isotropic, lossless medium with permittivity ε and permeability μ. For such a medium

$$\hat{\eta} = s\varepsilon\,, \tag{26.12-1}$$

$$\hat{\zeta} = s\mu\,, \tag{26.12-2}$$

and

$$\hat{\gamma} = s/c\,, \tag{26.12-3}$$

with

$$c = (\varepsilon\mu)^{-1/2}\,. \tag{26.12-4}$$

as the wave speed. Since the factor $\exp(-\hat{\gamma}|x|) = \exp(-s|x|/c)$ in the complex frequency domain corresponds in the time domain to a time delay of $|x|/c$, the time-domain equivalent of Equation (26.11-10) is (Figure 26.12-1)

$$\{E_k,H_j\}(x,t) = \frac{\{E_k^{\infty},H_j^{\infty}\}(\xi,t-|x|/c)}{4\pi|x|}\,[1+O(|x|^{-1})] \quad \text{as } |x|\to\infty\,, \tag{26.12-5}$$

where E_k^{∞} and H_j^{∞} follow from Equations (26.11-11) and (26.11-12) as

$$E_k^{\infty} = \mu(\xi_k\xi_r - \delta_{k,r})\partial_t\Phi_r^{J;\infty} + \varepsilon_{k,m,p}(\xi_m/c)\partial_t\Phi_p^{K;\infty}, \tag{26.12-6}$$

and

$$H_j^{\infty} = \varepsilon(\xi_j\xi_p - \delta_{j,p})\partial_t\Phi_p^{K;\infty} - \varepsilon_{j,n,r}(\xi_n/c)\partial_t\Phi_r^{J;\infty}. \tag{26.12-7}$$

In view of the property that the factor $\exp(\hat{\gamma}\xi_s x_s') = \exp(s\xi_s x_s'/c)$ in the complex frequency domain corresponds in the time domain to a time advance by the amount of $\xi_s x_s/c$, the time-domain equivalent of Equation (26.11-8)) is

$$\{\Phi_r^J,\Phi_p^K\}(x,t) = \{\Phi_r^{J;\infty},\Phi_p^{K;\infty}\}\frac{(\xi,t-|x|/c)}{4\pi|x|}\,[1+O(|x|^{-1})] \quad \text{as } |x|\to\infty\,, \tag{26.12-8}$$

in which, on account of Equation (26.11-9),

$$\{\Phi_r^{J;\infty},\Phi_p^{K;\infty}\}(\xi,t) = \int_{x'\in\mathcal{D}^T}\{J_r,K_p\}(x',t+\xi_s x_s'/c)\,\mathrm{d}V\,. \tag{26.12-9}$$

From this, we further obtain for their temporal derivative

$$\{\partial_t\Phi_r^{J;\infty},\partial_t\Phi_p^{K;\infty}\}(\xi,t) = \int_{x'\in\mathcal{D}^T}\{\partial_t J_r,\partial_t K_p\}(x',t+\xi_s x_s'/c)\,\mathrm{d}V\,. \tag{26.12-10}$$

As Equation (26.10-5) shows, the electric and the magnetic field strengths have, in the far-field region, the shape of a spherical wave that expands radially away from the chosen origin of the coordinate system (that is located in the neighbourhood of the sources and that is denoted as the reference centre of the far-field approximation), with an amplitude that depends on the direction of observation and that decreases inversely proportionally to the distance from the source to the point of observation. The amplitude radiation characteristics $\{E_k^{\infty},H_j^{\infty}\}$ depend only on the direction of observation ξ, and on the pulse shapes of the source distributions. The dependence on ξ is the resultant of the dependence on ξ of the integrals occurring in the right-hand sides of Equation (26.12-10) on ξ, and the electromagnetic far-field polar and axial radiation characteristics $\xi_k\xi_r - \delta_{k,r}$ and $-\varepsilon_{j,n,r}\xi_n$, respectively. Note that in the right-hand sides of Equations (26.12-6) and (26.12-7), via Equation (26.12-10), only the time-differentiated pulse shapes of the volume source current densities occur.

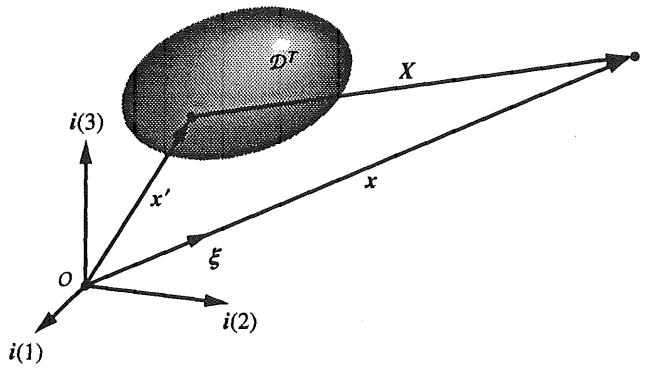

Figure 26.12-1 Far-field approximation to the distance function from source point $x' \in \mathcal{D}^T$ to observation point $x \in \mathcal{R}^3$: $|X| = |x - x'| = |x| - \xi_s x'_s + O(|x|^{-1})$ as $|x| \to \infty$.

The far-field amplitude radiation characteristics of the electric and the magnetic field strengths are not independent of each other. It is easily verified that the right-hand sides of Equations (26.10-6) and (26.10-7) are interrelated in the following way:

$$\varepsilon_{k,m,p}(\xi_m/c)H_p^\infty + \varepsilon E_k^\infty = 0\,, \tag{26.12-11}$$

$$-\varepsilon_{j,n,r}(\xi_n/c)E_r^\infty + \mu H_j^\infty = 0\,. \tag{26.12-12}$$

Now, relations of the kind of Equations (26.12-11) and (26.12-12) would also have resulted if expressions of the type

$$\{E_k, H_j\} = \{E_k^\infty, H_j^\infty\}(t - \xi_s x_s/c) \tag{26.12-13}$$

had been substituted in the source-free electromagnetic field equations pertaining to the homogeneous, isotropic, lossless medium under consideration and the causal relation between this wave field and its sources (that are located elsewhere in space), which entails zero initial values in time, had been used. Fields of the type of Equation (26.12-13) are denoted as *uniform electromagnetic plane waves*. Observing that $|x| = \xi_s x_s$, we can therefore say that, after compensating for the (distance)$^{-1}$ decay, the spherical-wave amplitudes in the far-field radiation pattern behave locally as if the wave were a plane wave travelling in the radial direction away from the source.

To exhibit the further properties of $\{E_k^\infty, H_j^\infty\}$ we rewrite Equations (26.12-11) and (26.12-12) as

$$\varepsilon_{k,m,p}\xi_m H_p^\infty + Y E_k^\infty = 0\,, \tag{26.12-14}$$

$$-\varepsilon_{j,n,r}\xi_n E_r^\infty + Z H_j^\infty = 0\,, \tag{26.12-15}$$

in which

$$Y = (\varepsilon/\mu)^{1/2} \tag{26.12-16}$$

is the *electromagnetic plane wave admittance* and

$$Z = (\mu/\varepsilon)^{1/2} \tag{26.12-17}$$

is the *electromagnetic plane wave impedance* of the medium under consideration. Contraction of Equation (26.12-14) with ξ_k and of Equation (26.12-15) with ξ_j leads to

$$\xi_k E_k^{\infty} = 0 \tag{26.12-18}$$

and

$$\xi_j H_j^{\infty} = 0\,, \tag{26.12-19}$$

respectively. Hence, the electric and the magnetic field strengths in the far-field region are transverse with respect to the local direction of propagation of the wave, and are, since $\varepsilon_{k,m,p}$ and ξ_m have unit magnitudes, proportional with proportionality factors Y or Z. Furthermore, E_k^{∞}, H_j^{∞} and ξ_s form a right-handed system of orthogonal vectors in each direction of observation in the far-field region.

Exercises

Exercise 26.12-1

Verify that Equations (26.12-6) and (26.12-7) indeed satisfy Equations (26.12-11) and (26.12-12).

Exercise 26.12-2

Let $F = F(x,t)$ be a tensor function of arbitrary rank, defined over some subdomain $\mathcal{D}$ of $\mathcal{R}^3$ and for all $t \in \mathcal{R}$. In addition, let $\partial_t F(x,t) = 0$ for all $x \in \mathcal{D}$ and all $t \in \mathcal{R}$, while $F(x,t_0) = 0$ for all $x \in \mathcal{D}$. Show that also $F(x,t) = 0$ for all $x \in \mathcal{D}$ and $t > t_0$. (*Hint*: Note that

$$0 = \int_{t'=t_0}^{t} \partial_{t'} F(x,t')\, \mathrm{d}t' = F(x,t) - F(x,t_0).$$

26.13 The time evolution of an electromagnetic wave field. The initial-value problem (Cauchy problem) for a homogeneous, isotropic, lossless medium

In this section a solution is presented for the initial-value problem (Cauchy problem) for an electromagnetic wave field in a homogeneous, isotropic, lossless medium with permittivity ε, permeability μ and electromagnetic wave speed $c = (\varepsilon\mu)^{-1/2}$. From the given initial values $E_k(x,t_0)$ of the electric field strength and $H_j(x,t_0)$ of the magnetic field strength in all space at the instant t_0, the values of $E_k = E_k(x,t)$ and $H_j = H_j(x,t)$ at all succeeding instants $t > t_0$ are to be constructed in case nowhere in the medium sources are active for $t \geqslant t_0$. Thus, we are looking for the pure time evolution for $t > t_0$ of the electromagnetic wave field, given its values of the electric and the magnetic field strengths at $t = t_0$. From Equations (24.1-3) and (24.1-4) we learn that this problem can be solved by transforming Equations (26.3-1)–(26.3-5), back to the time domain for the particular case where

$$\hat{J}_r = -\varepsilon E_r(x,t_0)\exp(-st_0)\,, \tag{26.13-1}$$

and

$$\hat{K}_p = -\mu H_p(x,t_0)\exp(-st_0)\,. \tag{26.13-2}$$

Substitution of Equations (26.13-1) and (26.13-2) in Equations (26.3-3) and (26.3-4) leads to

$$\hat{\Phi}_r^J(x,s) = -\varepsilon \int_{x'\in\mathcal{R}^3} E_r(x',t_0)\,\frac{\exp\,[-s|x-x'|/c - st_0]}{4\pi|x-x'|}\,\mathrm{d}V \tag{26.13-3}$$

and

$$\hat{\Phi}_p^K(x,s) = -\mu \int_{x'\in\mathcal{R}^3} H_p(x',t_0)\,\frac{\exp\,[-s|x-x'|/c - st_0]}{4\pi|x-x'|}\,\mathrm{d}V\,. \tag{26.13-4}$$

The integrals on the right-hand sides of Equations (26.13-3) and (26.13-4) will be rewritten such that their time-domain counterparts can be obtained by inspection. This is accomplished by introducing spherical polar coordinates about the observation point x as the variables of integration. Consider, to this end, the generic expression

$$\hat{\Phi}(x,s) = \int_{x'\in\mathcal{R}^3} q(x',t_0)\,\frac{\exp\,[-s|x-x'|/c - st_0]}{4\pi|x-x'|}\,\mathrm{d}V\,. \tag{26.13-5}$$

On the right-hand side, $c(\tau - t_0)$, with $\tau \geqslant t_0$, is now taken as the radial variable of integration and the unit vector θ with $\theta\in\Omega$, where Ω denotes the sphere of unit radius, as the angular variable of integration. Then,

$$x' = x + c(\tau - t_0)\theta\,, \tag{26.13-6}$$

and, since $\theta_m\theta_m = 1$,

$$|x-x'| = c(\tau - t_0)\,, \tag{26.13-7}$$

and hence

$$|x-x'|/c + t_0 = \tau\,, \tag{26.13-8}$$

while

$$\mathrm{d}V = c^3(\tau - t_0)^2\,\mathrm{d}\tau\,\mathrm{d}\Omega\,, \tag{26.13-9}$$

where $\mathrm{d}\Omega$ is the elementary area on Ω. With this, Equation (26.13-5) is rewritten as

$$\hat{\Phi}(x,s) = \int_{\tau=t_0}^{\infty} \exp(-s\tau)c^2(\tau - t_0)\langle q(x',t_0)\rangle_{S[x,c(\tau-t_0)]}\,\mathrm{d}\tau\,, \tag{26.13-10}$$

in which

$$\langle q(x',t_0)\rangle_{S[x,c(\tau-t_0)]} = \frac{1}{4\pi}\int_{\theta\in\Omega} q\,[x + c(\tau - t_0)\theta, t_0]\,\mathrm{d}\Omega \tag{26.13-11}$$

denotes the spherical mean over the sphere $S[x;c(\tau - \tau_0)]$ with its centre at x and radius $c(\tau - t_0)$.

Now, the right-hand side of Equation (26.13-10) has the form of the Laplace transformation of a causal function of time whose support is $\{t\in\mathcal{R};t > t_0\}$. In view of the uniqueness of the Laplace transformation with real, positive transform parameter (see Section B.1), the time-domain counterpart $\Phi(x,t)$ of $\hat{\Phi}(x,s)$ is given by

$$\Phi(x,t) = c^2(t-t_0)\langle q(x',t_0)\rangle_{S[x,c(t-t_0)]} \qquad \text{for } t \geq t_0 . \tag{26.13-12}$$

Using this generic result, the time-domain counterparts of Equations (26.13-3) and (26.13-4) are obtained as

$$\Phi_r^J(x,t) = -\varepsilon c^2(t-t_0)\langle E_r(x',t_0)\rangle_{S[x,c(t-t_0)]} \qquad \text{for } t \geq t_0 \tag{26.13-13}$$

and

$$\Phi_p^K(x,t) = -\mu c^2(t-t_0)\langle H_p(x',t_0)\rangle_{S[x,c(t-t_0)]} \qquad \text{for } t \geq t_0 . \tag{26.13-14}$$

In terms of these source vector potentials the expressions for the electric and the magnetic field strengths follow from Equations (26.4-7) and (26.4-8) as

$$E_k(x,t) = -\mu\partial_t\Phi_k^J + \varepsilon^{-1}\partial_k\partial_r I_t\Phi_r^J - \varepsilon_{k,m,p}\partial_m\Phi_p^K \qquad \text{for } t \geq t_0 , \tag{26.13-15}$$

and

$$H_j(x,t) = -\varepsilon\partial_t\Phi_j^K + \mu^{-1}\partial_j\partial_p I_t\Phi_p^K + \varepsilon_{j,n,r}\partial_n\Phi_r^J \qquad \text{for } t \geq t_0 . \tag{26.13-16}$$

Equations (26.13-13)–(26.13-16) constitute the solution to the electromagnetic initial-value problem and govern the time evolution of an electromagnetic field in a homogeneous, isotropic, lossless medium.

Exercises

Exercise 26.13-1

Construct the solution to the initial-value problem (Cauchy problem) of the three-dimensional scalar wave equation

$$\partial_m\partial_m u - c^{-2}\partial_t^2 u = 0 \tag{26.13-17}$$

for $t > t_0$ if $u(x,t_0) = u_0(x)$ and $\partial_t u(x,t_0) = v_0(x)$.

(a) Take the time Laplace transform of Equation (26.13-17) over the interval $t_0 < t < \infty$ and show that

$$\partial_m\partial_m\hat{u} - (s^2/c^2)\,\hat{u} = -c^{-2}v_0(x)\exp(-st_0) - c^{-2}su_0(x)\exp(-st_0) . \tag{26.13-18}$$

(b) Show that the solution to Equation (26.13-18) is given by

$$\hat{u}(x,s) = \int_{x'\in\mathcal{R}^3}\hat{q}(x')\,\frac{\exp[-s|x-x'|/c - st_0]}{4\pi|x-x'|}\,dV , \tag{26.13-19}$$

in which

$$\hat{q}(x') = c^{-2}[v_0(x') + su_0(x')] . \tag{26.13-20}$$

(c) Introduce spherical polar coordinates about the observation point x as the variables of integration and show that

$$\hat{u}(x,s) = \int_{\tau=t_0}^{\infty} \exp(-s\tau)(\tau - t_0)\langle v_0(x')\rangle_{S[x,c(\tau-t_0)]}\,\mathrm{d}\tau + s\int_{\tau=t_0}^{\infty} \exp(-s\tau)(\tau - t_0)\langle u_0(x')\rangle_{S[x,c(\tau-t_0)]}\,\mathrm{d}\tau\,, \tag{26.13-21}$$

in which

$$\langle u_0(x')\rangle_{S[x,c(\tau-t_0)]} = \frac{1}{4\pi}\int_{\theta\in\Omega} u_0[x + c(\tau - t_0)\theta]\,\mathrm{d}\Omega \tag{26.13-22}$$

is the spherical mean over the sphere $S[x,c(\tau - t_0)]$ with its centre at x and radius $c(\tau - t_0)$.
(d) Use the uniqueness of the time Laplace transformation to show that

$$u(x,t) = (t - t_0)\langle v_0(x')\rangle_{S[x,c(t-t_0)]} + \partial_t\left\{(t - t_0)\langle u_0(x')\rangle_{S[x,c(t-t_0)]}\right\} \quad \text{for } t \geqslant t_0\,. \tag{26.13-23}$$

Equation (26.13-23) is Poisson's solution to the initial-value problem of the three-dimensional scalar wave equation.

References

Abramowitz, M. and Stegun, I.E., 1964a, *Handbook of Mathematical Functions*, Washington DC: National Bureau of Standards, Formula 9.6.16, p. 376.

Abramowitz, M. and Stegun, I.E., 1964b, *Handbook of Mathematical Functions*, Washington, DC: National Bureau of Standards, Formula 9.6.27, p. 376.

Abramowitz M. and Stegun, I.E., 1964c, *Handbook of Mathematical Functions*, Washington D.C: National Bureau of Standards, Formula 9.1.18, p. 360.

Abramowitz M. and Stegun, I.E., 1964d, *Handbook of Mathematical Functions*, Washington D.C: National Bureau of Standards, Formula 9.1.28, p. 361.